

*Spatial variations in CO<sub>2</sub> fluxes in a subtropical coastal reservoir of Southeast China were related to urbanization and land-use types*

Article

Accepted Version

Creative Commons: Attribution-Noncommercial-No Derivative Works 4.0

Zhang, Y., Lyu, M., Yang, P., Lai, D. Y. F., Tong, C., Zhao, G., Li, L., Zhang, Y. and Yang, H. ORCID: <https://orcid.org/0000-0001-9940-8273> (2021) Spatial variations in CO<sub>2</sub> fluxes in a subtropical coastal reservoir of Southeast China were related to urbanization and land-use types. *Journal of Environmental Sciences*, 109. pp. 206-218. ISSN 1001-0742 doi: 10.1016/j.jes.2021.04.003 Available at <https://centaur.reading.ac.uk/97922/>

It is advisable to refer to the publisher's version if you intend to cite from the work. See [Guidance on citing](#).

To link to this article DOI: <http://dx.doi.org/10.1016/j.jes.2021.04.003>

Publisher: Elsevier

All outputs in CentAUR are protected by Intellectual Property Rights law, including copyright law. Copyright and IPR is retained by the creators or other copyright holders. Terms and conditions for use of this material are defined in

the [End User Agreement](#).

[www.reading.ac.uk/centaur](http://www.reading.ac.uk/centaur)

## **CentAUR**

Central Archive at the University of Reading

Reading's research outputs online

1 **Spatial variations in CO<sub>2</sub> fluxes in a subtropical coastal reservoir**  
2 **of Southeast China were related to urbanization and land-use**  
3 **types**

4  
5 **Yifei Zhang<sup>1,2,3</sup>, Min Lyu<sup>4</sup>, Ping Yang<sup>1,2\*</sup>, Derrick Y.F. Lai<sup>5</sup>, Chuan Tong<sup>1,2,\*\*</sup>, Guanghui**  
6 **Zhao<sup>2</sup>, Ling Li<sup>2</sup>, Yuhan Zhang<sup>2</sup>, Hong Yang<sup>6,7,8,\*\*\*</sup>**

7  
8 *<sup>1</sup>Key Laboratory of Humid Subtropical Eco-geographical Process of Ministry of Education, Fujian*  
9 *Normal University, Fuzhou 350007, P.R. China*

10 *<sup>2</sup>School of Geographical Sciences, Fujian Normal University, Fuzhou 350007, P.R. China*

11 *<sup>3</sup>Key Laboratory of Wetland Ecology and Environment, Northeast Institute of Geography and*  
12 *Agroecology, Chinese Academy of Sciences, Changchun 130102, Jilin, P.R. China*

13 *<sup>4</sup>School of Urban and Rural Construction, Shaoyang University, Shaoyang 422000, China*

14 *<sup>5</sup>Department of Geography and Resource Management, The Chinese University of Hong Kong, Hong*  
15 *Kong, China*

16 *<sup>6</sup>College of Environmental Science and Engineering, Fujian Normal University, Fuzhou 350007,*  
17 *P.R. China*

18 *<sup>7</sup>Collaborative Innovation Center of Atmospheric Environment and Equipment Technology, Jiangsu*  
19 *Key Laboratory of Atmospheric Environment Monitoring and Pollution Control (AEMPC), School of*  
20 *Environmental Science and Engineering, Nanjing University of Information Science and Technology,*  
21 *Nanjing, 210044, China*

22 *<sup>8</sup>Department of Geography and Environmental Science, University of Reading, Reading, RG6 6AB*  
23 *UK*

24 **\*Corresponding authors:** Ping Yang (yangping528@sina.cn)

25 **\*\*Corresponding authors:** Chuan Tong (tongch@fjnu.edu.cn)

26 **Telephone:** 086-0591-87445659 **Fax:** 086-0591-83465397 **Email:** [tongch@fjnu.edu.cn](mailto:tongch@fjnu.edu.cn)

27 **\*\*\*Corresponding authors:** Hong Yang (hongyanghy@gmail.com)

28

29 **Abstract**

30 Carbon dioxide (CO<sub>2</sub>) emissions from aquatic ecosystems are important components of the  
31 global carbon cycle, yet the CO<sub>2</sub> emissions from coastal reservoirs, especially in developing  
32 countries where urbanization and rapid land use change occur, are still poorly understood. In  
33 this study, the spatiotemporal variations in CO<sub>2</sub> concentrations and fluxes were investigated  
34 in Wenwusha Reservoir located in the southeast coast of China. Overall, the mean  
35 CO<sub>2</sub> concentration and flux across the whole reservoir were  $41.85 \pm 2.03 \mu\text{mol/L}$  and  $2.87 \pm$   
36  $0.29 \text{ mmol/m}^2/\text{h}$ , respectively, and the reservoir was a consistent net CO<sub>2</sub> source over the  
37 entire year. The land use types and urbanization levels in the reservoir catchment  
38 significantly affected the input of exogenous carbon to water. The mean CO<sub>2</sub> flux was much  
39 higher from waters adjacent to the urban land ( $5.05 \pm 0.87 \text{ mmol/m}^2/\text{hr}$ ) than other land use  
40 types. Sites with larger input of exogenous substance via sewage discharge and upstream  
41 runoff were often the hotspots of CO<sub>2</sub> emission in the reservoir. Our results suggested that  
42 urbanization process, agricultural activities, and large input of exogenous carbon could result  
43 in large spatial heterogeneity of CO<sub>2</sub> emissions and alter the CO<sub>2</sub> biogeochemical cycling in  
44 coastal reservoirs. Further studies should characterize the diurnal variations, microbial  
45 mechanisms, and impact of meteorological conditions on reservoir CO<sub>2</sub> emissions to expand  
46 our understanding of the carbon cycle in aquatic ecosystems.

47 **Keywords**

48 Carbon dioxide fluxes; Spatiotemporal dynamics; Land use; Urbanization; Anthropogenic  
49 activities; Coastal reservoir

50

## 51 Introduction

52 Dams have been built for thousands of years to control water flow and utilize water resources  
53 (Nilsson et al., 2005). As an artificial aquatic ecosystem, reservoirs play an important role in  
54 irrigation, water supply, power generation, aquaculture and other aspects, while the impacts  
55 of such water projects on the local hydrological situation and ecosystem sustainability have  
56 not been fully explored (Hao et al., 2019; Rosenberg et al., 2000). With the inundation of  
57 land and vegetation in the reservoir area, nutrient transport and cycling in the flooded system  
58 will change substantially, with the consequence of changing the emission of greenhouse  
59 gases (GHGs), including CO<sub>2</sub>, CH<sub>4</sub> and N<sub>2</sub>O, into the atmosphere (Li et al., 2016; St Louis  
60 et al., 2000). Therefore, with the exacerbating climate change caused by increasing GHG  
61 concentrations (World Meteorological Organization, 2019), quantifying the carbon flux of  
62 reservoirs becomes increasingly important to improve the accuracy of carbon budget  
63 estimations from local to global scales.

64 Artificial reservoir, which includes various carbon sources from the catchment and inside the  
65 reservoir, is a major component of global carbon cycle (Bevelhimer et al., 2016; Kunz et al.,  
66 2011). Recent estimate indicates that global GHG emissions from reservoir water surfaces  
67 account to approximately 0.8 Pg CO<sub>2</sub>-eq (100-year) per year, of which ~17% is contributed  
68 by CO<sub>2</sub> (Deemer et al., 2016). Reservoirs appear to be a net source of atmospheric  
69 CO<sub>2</sub> (Barros et al., 2011; Raymond et al., 2014), especially in the subtropical and tropical  
70 areas (e.g., Alshboul and Lorke, 2015; Almeida et al., 2019). CO<sub>2</sub> emissions from reservoirs  
71 on a per unit area basis tend to exceed those from natural lakes or wetlands. However, limited  
72 by the number of field observations available, these CO<sub>2</sub> estimates are largely uncertain  
73 (Li and Lu, 2012; Varis et al., 2012). More importantly, the spatial heterogeneity (across and  
74 within systems) caused by geographical location, reservoir age, microtopography, water  
75 temperature, organic matter, and other factors further pose challenges for the accurate  
76 estimate of CO<sub>2</sub> emissions from reservoirs.

77 Different from other natural water bodies, reservoirs have special ecosystem characteristics  
78 under the intervention of human activities (Fearnside, 2005; Soumis et al., 2007). Generally,  
79 the inundated sediment, suspended particles and other associated carbon trapped in reservoirs  
80 provide stable carbon sources for CO<sub>2</sub> production, but with large spatial heterogeneity  
81 (Hertwich, 2013; Kemenes et al., 2011; Zhou et al., 2017). On the other hand, some eutrophic  
82 waters with higher primary productivity can fix a large amount of CO<sub>2</sub>, and even serve as a  
83 carbon sink for a certain period (Pacheco et al., 2015). Previous studies suggested several  
84 possible conditions for the dominance of autotrophic processes: (1) relatively enclosed and  
85 stagnant water environment (van Bergen et al., 2019); (2) warm and humid climate  
86 (Barros et al., 2011; Xiao et al., 2017); and (3) excessive import and accumulation of  
87 nutrients and organic matter in the reservoirs (Dodds and Cole, 2007; Outram and  
88 Hiscock, 2012). Furthermore, compared with inland areas, coastal reservoirs trend to have a  
89 higher salinity (Domingues et al., 2016; Hodson et al., 2019). CO<sub>2</sub> production and emission  
90 may also exhibit some spatial differences owing to variations in salinity.

91 With rapid urbanization and land use change in the coastal areas, various biogeochemical  
92 processes in the coastal aquatic ecosystems have been increasingly disturbed by municipal  
93 and agricultural activities in the catchment (Pérez et al., 2015; Williams et al., 2016), leading  
94 to the creation of critical “hotspots” of GHG emission (Yang and Flower 2012). High  
95 CO<sub>2</sub> production and emission in some river and lake systems have been shown to closely  
96 relate to the exogenous supply of sewage-derived organic matter from the watershed (e.g.,  
97 Kaushal et al., 2018; Pugh et al., 2015). Coastal reservoirs, which can be affected by both  
98 terrestrial and marine ecosystems, are likely to exhibit unique CO<sub>2</sub> dynamics. Given that most

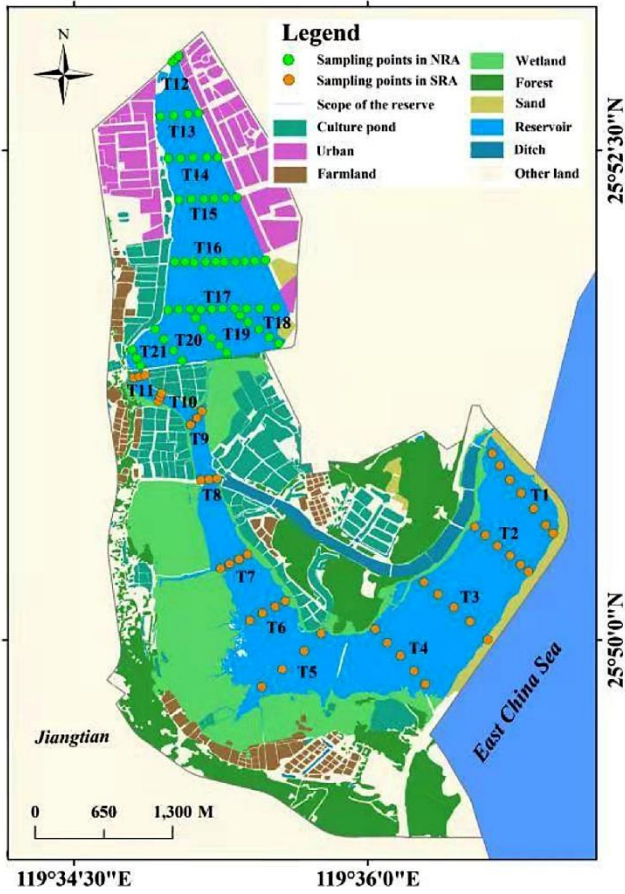
99 of the existing studies on CO<sub>2</sub> fluxes in reservoirs are mainly devoted to inland hydroelectric  
100 reservoirs only (e.g., Abril et al., 2005; Shi et al., 2017) but rapid urbanization occurs widely  
101 in the catchment of coastal reservoirs, particularly in the developing countries (Yang et al.,  
102 2017). Therefore, a deeper understanding about the influence of land use change and  
103 urbanization on CO<sub>2</sub> fluxes in the coastal reservoirs is needed.

104 Given the knowledge gap above, we measured CO<sub>2</sub> concentrations and fluxes in a subtropical  
105 coastal reservoir in Min River Estuary, Southeast China, from November 2018 to June 2019.  
106 The goals of this study were: (1) to assess the spatial variability of CO<sub>2</sub> concentration and  
107 flux in the subtropical coastal reservoir system, and (2) to determine the response of reservoir  
108 CO<sub>2</sub> release to the adjacent land use types. We hypothesized a large spatial heterogeneity in  
109 reservoir CO<sub>2</sub> fluxes because of the different land use types and urbanization levels in the  
110 catchment.

## 111 **1. Materials and methods**

### 112 **1.1. Site description**

113 This study was conducted in Wenwusha Reservoir (25°49'36"–25°54'00"N,  
114 119°35'12"–119°38'11"E), which was located at the southern tip of the Min River Estuary,  
115 Southeast China (**Fig. 1**). The reservoir catchment is influenced by a subtropical monsoon  
116 climate with high temperature (annual average: 19.3 °C) and abundant precipitation (annual  
117 average: 1390 mm). Nearly 75% of the annual precipitation occurs from May to September  
118 (Yang et al., 2020). The reservoir water meets China's Class III water quality standard  
119 (suitable for centralized drinking water source protection zone, fish protection zone and  
120 swimming zone), and the reservoir is mainly used for irrigation, aquaculture and flood  
121 control (Fuzhou Municipal Water Authorities, 2019). Different species of fish,  
122 including *Lateolabrax japonicus*, *Oreochromis mossambicus*, *Carassius auratus*  
123 *auratus* and *Cyprinus carpio*, grow in the reservoir. The main land uses adjacent to the  
124 reservoir are urban area (5.99%), aquaculture pond (9.80%), forest (15.04%), farmland  
125 (3.34%), sand (2.14%) and wetland (14.41%) (**Fig. 1** and **Table 1**).



126

127

128

129

130

Fig. 1. Location of the Wenwusha Reservoir and land use distribution in the catchment. There are 11 sample transects (47 sampling sites) in the south reservoir area (SRA) and 10 sampling transects (56 sampling sites) in the north reservoir area (NRA).

131 **Table 1**

132 Summary of main characteristics and land use types in the Wenwusha Reservoir

	Surface area	Total volume	Water depth	Bank type <sup>a</sup>	Sampling Site	Land use type (%)					
	(ha)	( $\times 10^8$ m <sup>3</sup> )	(m)			Urban	Pond	Farmland	Wetland	Forest	Sand
NRA	190	1.4	2.6	N/C	56	23.93	6.30	2.01	0.01	0.34	1.41
SRA	330	1.69	1.2	N	47	0.00	10.96	3.78	10.96	19.94	2.39

133 <sup>a</sup>“N” and “C” represent natural and concreted banks. NRA and SRA are north reservoir area and sour reservoir area.

134

135 The total reservoir water area and mean water depth are 520 ha and 1.5 m, respectively. Two  
136 dams were built in 1957 and 2004, respectively, which divided the reservoir into two main  
137 reservoir areas: north reservoir area (NRA) and south reservoir area (SRA) (**Fig. 1**). The  
138 NRA, with a surface area of 190 ha, is connected to the Nanyang River network. Influenced  
139 by urbanization and human activities, the NRA and its upstream receive effluent discharge  
140 from domestic, industrial and aquacultural activities (**Table 1**). The construction of the  
141 southern seawall resulted in the SRA, with a surface area of 330 ha. Trees were planted in the  
142 east of SRA, while extensive wetlands were formed along the west bank of SRA with some  
143 agricultural landscapes (e.g., aquaculture ponds and farmlands) (**Table 1**). Water in the whole  
144 reservoir is supplied by precipitation and upstream river discharge, with almost no exchange  
145 with sea.

## 146 **1.2. Water sampling and CO<sub>2</sub> measurement**

147 Considering the possible spatiotemporal variations in dissolved CO<sub>2</sub> concentration and flux,  
148 three sampling campaigns (November 2018, March and June 2019) were carried out across  
149 21 sampling transects (103 sites) at the Wenwusha reservoir, including 10 sampling transects  
150 in NRA (56 sites) and 11 transects in SRA (47 sites). Moreover, according to different levels  
151 of urbanization along the reservoir bank in the catchment, the reservoir was further divided  
152 into four water areas (I, II, III, and IV) (Appendix A **Table S1**). The sampling points  
153 basically covered all the water areas with the dominating land use types in the catchment  
154 (**Fig. 1**). The coordinates of each sampling site were recorded so that the same sites were re-  
155 visited in all three sampling campaigns. Water samples were collected using 55-mL  
156 borosilicate serum bottles (~0.2 m below the water surface), which were then sealed with  
157 butyl stoppers and aluminum caps without including any bubbles. In addition, 150-mL of  
158 water sample was collected at each site using a polyvinylchloride sampling bottle for the  
159 measurement of other auxiliary parameters (see below).

160 CO<sub>2</sub> concentration was determined using the headspace extraction technique (Bellido et al.,  
161 2009). Specifically, 25 mL of water sample and equal volume of N<sub>2</sub> were added into a bottle  
162 and the bottle was then violently shaken for 10 min to reach an equilibrium in  
163 CO<sub>2</sub> concentration. 5 mL of headspace air sample was collected and subsequently injected  
164 into a gas chromatograph (GC-2010, Shimadzu, Kyoto, Japan) with flame ionization  
165 detection (FID) for determining the CO<sub>2</sub> concentration. Four CO<sub>2</sub> standard gases, i.e. 100,  
166 500, 1000 and 10,000 ppm, were used to calibrate the FID. The injection port, column and  
167 detector temperature were set at 100, 45 and 240 °C, respectively. Dissolved  
168 CO<sub>2</sub> concentration in water was calculated following the method of Wanninkhof (1992),  
169 based on the CO<sub>2</sub> concentration in the headspace air in the serum bottle and the Bunsen  
170 solubility coefficient.

171 The CO<sub>2</sub> flux ( $F_{CO_2}$ ) across the water-air interface was estimated using the thin-boundary  
172 layer model based on gas diffusion between two media (e.g., Crawford et al., 2013) as  
173 follows: (1)  $F_{CO_2} = k \cdot (C_{water} - C_{atm})$  where  $F_{CO_2}$  (mmol/m<sup>2</sup>/h) refers to the CO<sub>2</sub> flux from  
174 water to air;  $k$  is the gas transfer velocity of CO<sub>2</sub> (m/hr);  $C_{water}$  is the CO<sub>2</sub> concentration in the  
175 water column (mmol/L), and  $C_{atm}$  is the CO<sub>2</sub> concentration in the atmosphere (mmol/L). In the  
176 lentic system, according to the empirical function driven by wind speed and temperature  
177 (Crusius and Wanninkhof, 2003), the  $k$  value can be calculated  
178 as: (2)  $k = (1.68 + 0.228 \cdot U_{10}^{0.2}) \cdot (600 S_c)^n$  (3)  $S_c = 1991.1 - 118.11t + 3.4527t^2 - 0.04132t^3$  where  
179  $U_{10}$  (m/sec) is the wind speed at 10 m above the water surface, which is approximated by  $U_{10} =$   
180  $1.14 U$ , where  $U$  is the wind speed at 2 m height;  $S_c$  is the CO<sub>2</sub> Schmidt number for water  
181 temperature ( $t$ , °C) (Wanninkhof, 1992); and  $n$  is the proportionality coefficient (value is 0.5).

### 182 **1.3. Field and laboratory measurement of water physico-chemical properties**

183 During the sampling period, various physio-chemical properties of surface water were also  
184 measured *in situ*. Water temperature ( $T_w$ ) and pH were measured by a portable  
185 pH/mV/temperature meter system (IQ150 Scientific Instruments, USA). Dissolved oxygen  
186 (DO) and salinity were determined by a portable water quality analyzer (HORIBA, Japan)  
187 and a salinity meter (Eutech Instruments-Salt6, USA), respectively. The relative standard  
188 deviations of pH, DO, and salinity analyses were  $\leq 1.0\%$ ,  $\leq 2.0\%$  and  $\leq 1.0\%$ , respectively.  
189 All equipment probes were calibrated following the manufacturer's specifications prior to  
190 deployment. Meteorological conditions (including wind speed, air pressure and temperature)  
191 were measured by a meteorological meter (NK3500, Kestrel, USA), and long-term  
192 precipitation data were obtained from the weather stations in Min River Estuary.

193 Laboratory analyses were conducted to determine the nutrient concentrations in reservoir  
194 water. Before the analysis of dissolved nutrients, water samples were filtered through 0.45–  
195  $\mu\text{m}$  GF/F glass millipore filters. Dissolved organic carbon (DOC) concentration was analyzed  
196 by a total organic carbon analyzer (TOC-VCPH/CPN, Shimadzu, Japan) with a detection  
197 limit of 0.4  $\mu\text{g/L}$  and a relative standard deviation (RSD) of  $\leq 1.0\%$  in 24 h. Nitrogen (total  
198 dissolved nitrogen (TDN),  $\text{NO}_3^-$ , and  $\text{NH}_4^+$ ) and phosphorus (total phosphorus (TP) and  $\text{PO}_4^{3-}$ )  
199 nutrients were detected using flow injection analyzer (Skalar Analytical SAN<sup>++</sup>, Netherlands).  
200 The detection limits for nitrogen and phosphorus were 6  $\mu\text{g/L}$  and 3  $\mu\text{g/L}$ , respectively, and  
201 the measurement reproducibilities were within 3.0% and 2.0%, respectively.  
202 Chlorophyll *a* (Chl-*a*) was extracted using ethanol solution (90%) for 24 h and analyzed by a  
203 UV–VIS spectrophotometer (Shimadzu UV-2450, Japan).

### 204 **1.4. Statistical analysis**

205 All measured variables were checked for normality using the Kolmogorov-Smirnov's test.  
206 When necessary, the original data were transformed by the natural logarithm to meet the  
207 assumptions of normality and homoscedasticity. To fully consider the correlation between  
208 spatial variables, as well as the randomness and structural characteristics of the spatial  
209 distribution of samples, the Kriging method in ArcGIS 10.2 (Esri, Redland, CA, USA) was  
210 employed for the spatial interpolation. Significant differences in  $\text{CO}_2$  concentration, flux and  
211 environmental variables among different water areas were tested by analysis of variance  
212 (ANOVA). Spearman correlation and simple regression analysis were conducted to explore  
213 the relationships between  $\text{CO}_2$  concentration (or flux) and the physio-chemical properties of  
214 water. Statistical significance was examined at the level of 0.05. The key factors influencing  
215 the  $\text{CO}_2$  concentration and flux in the two reservoir areas were further investigated using  
216 redundancy analysis (RDA) in CANOCO 5.0 (Ithaca, NY, USA). Statistical results and  
217 graphics were generated by using SPSS 17.0 (IBM, Chicago, IL, USA) and Origin 2017  
218 (OriginLab Corporation, USA), separately.

## 219 **2. Results**

### 220 **2.1. Meteorological conditions and physico-chemical properties of reservoir** 221 **water**

222 The general spatiotemporal variations of surface water physico-chemical properties have  
223 been reported in Yang et al. (2020) (**Table 2** and Appendix A **Fig. S2**), while in this study,  
224 we focused on the effects of urbanization. Daily temperature, atmospheric pressure, wind  
225 speed, water salinity and Chl-*a* concentration showed small spatial variations, and the mean  
226 difference was less than 4 °C, 10 hPa, 3 m/s, 2‰ and 9  $\mu\text{g/L}$ , respectively, during the  
227 research period. Spatially, water DO, TOC, TDN,  $\text{NH}_4^+$ , and  $\text{PO}_4^{3-}$  concentration varied

228 considerably among the four areas. TOC,  $\text{NH}_4^+$  and TDN in Areas I and Area-II showed  
229 much higher concentrations than those in Area-III and Area-IV ( $p < 0.05$  or  
230 0.01; **Table 2** and Appendix A **Fig. S2**), with the highest values usually observed in Area-I.  
231 In most of the time, DO concentrations increased in the order: Area-I < Area-III < Area-II <  
232 Area-IV. However, in March, DO concentrations in Area-II were higher than those in other  
233 three areas (**Table 2** and Appendix A **Fig. S2**).

234

235 **Table 2**

236 Summary of the two-way ANOVA results determining the effect of sampling water areas, seasons, and their interactions on water environmental variables in  
 237 Wenwusha Reservoir

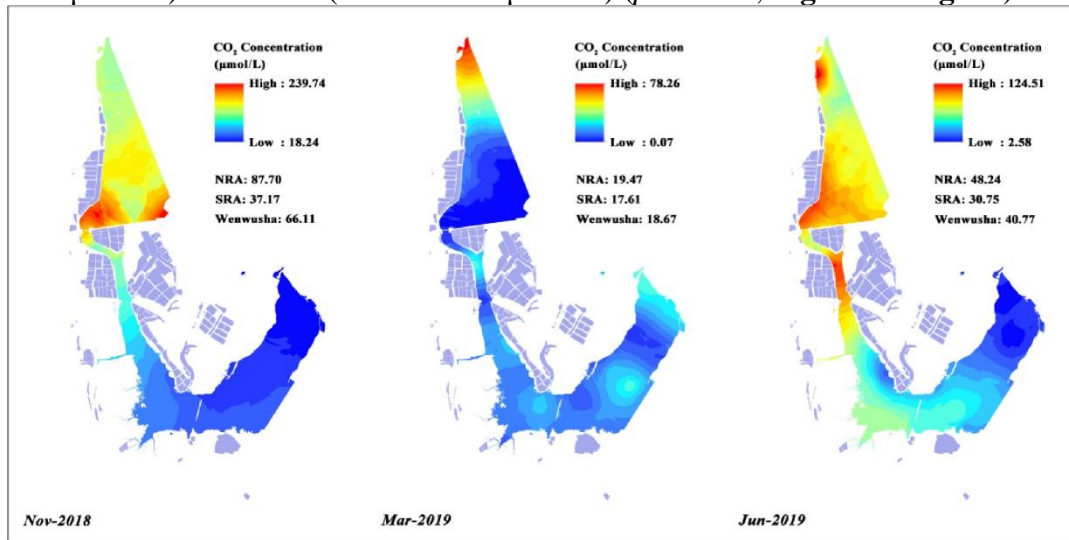
	<i>df</i>	pH	DO	TOC	NH <sub>4</sub> <sup>+</sup>	TDN	PO <sub>4</sub> <sup>3-</sup>
Sampling area	3	17.00**	201.52**	1078.99**	22.02**	85.31**	7.368**
Season	2	1046.31**	1046.16**	2.37	32.65**	19.91**	14.953**
Sampling area × Season	6	11.64**	115.55**	4.78**	1.14	29.72**	9.012**

238 Symbols \* and \*\* indicate significant differences at 0.05 and 0.01, respectively.

239 In general, sampling sites around human-dominated landscapes (residential  
 240 area, aquaculture pond, and farmland) in NRA in the Wenwusha reservoir had higher nutrient  
 241 levels (i.e. TOC, TDN, and  $\text{NH}_4^+$  concentration), pH value and Chl-*a* concentrations but  
 242 lower DO concentrations than those near the natural landscapes, such as wetland and forest in  
 243 SRA.

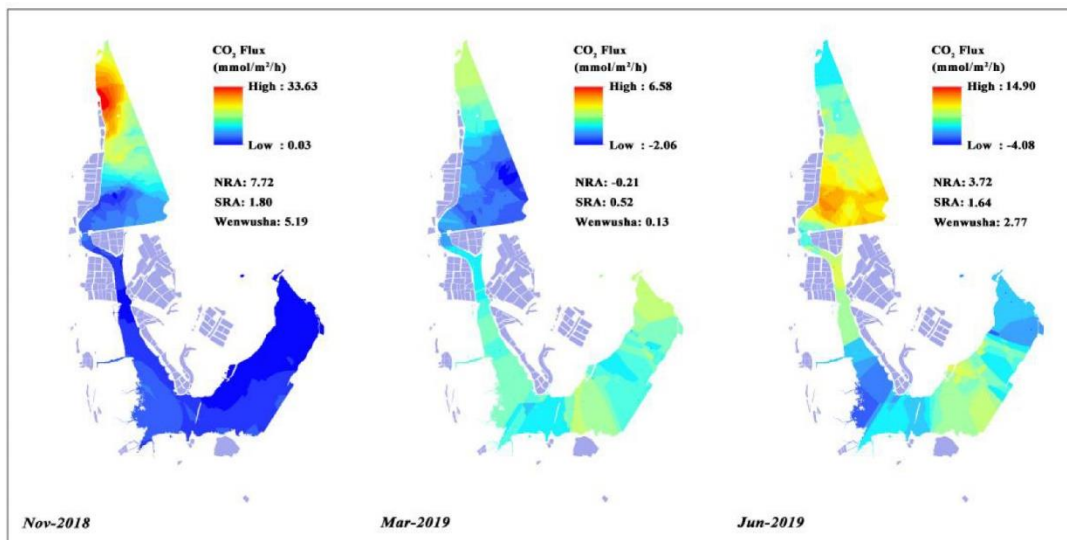
## 244 2.2. Spatial variation in $\text{CO}_2$ dynamics across four water areas

245 During the sampling period, large spatial variations in  $\text{CO}_2$  concentrations were observed  
 246 across different areas. Dissolved  $\text{CO}_2$  concentrations in Area-I, Area-II, Area-III, and Area IV  
 247 varied over the ranges of 1.80–178.26  $\mu\text{mol/L}$ , 0.07–239.74  $\mu\text{mol/L}$ , 3.21–59.17  $\mu\text{mol/L}$ , and  
 248 1.02–64.91  $\mu\text{mol/L}$ , respectively. Dissolved  $\text{CO}_2$  concentrations decreased significantly in the  
 249 order: Area-I ( $52.89 \pm 3.64 \mu\text{mol/L}$ ) > Area-II ( $49.22 \pm 2.95 \mu\text{mol/L}$ ) > Area-III ( $29.51 \pm$   
 250  $2.88 \mu\text{mol/L}$ ) > Area-IV ( $22.03 \pm 1.53 \mu\text{mol/L}$ ) ( $p < 0.001$ , **Fig. 2** and **Fig. 4a**).



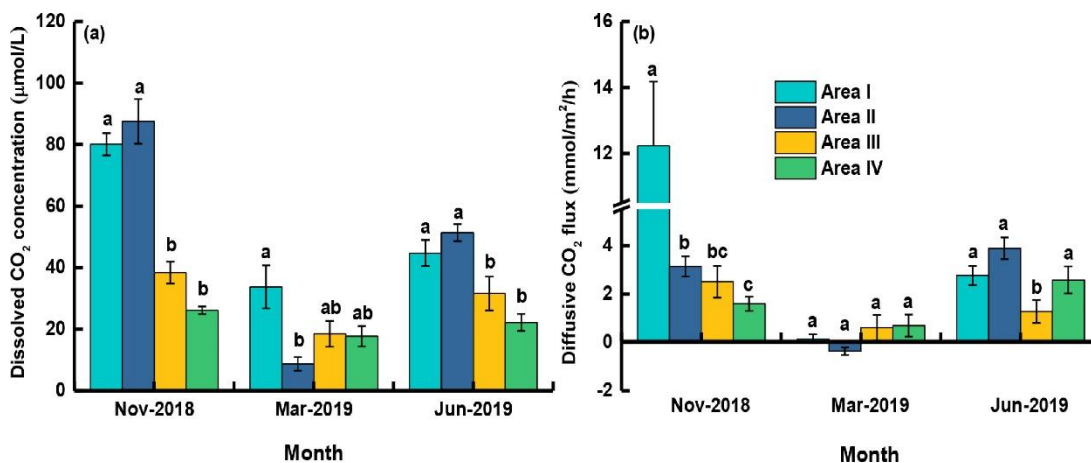
251  
 252 Fig. 2. Spatial distribution of dissolved  $\text{CO}_2$  concentrations in surface water ( $\sim 0.2$  m depth)  
 253 of Wenwusha Reservoir from November 2018 to June 2019.

254 Across the three sampling campaigns,  $\text{CO}_2$  fluxes across the water-air interface decreased in  
 255 the order: Area-I ( $5.05 \pm 0.87 \text{ mmol/m}^2/\text{hr}$ ) > Area-II ( $2.22 \pm 0.27 \text{ mmol/m}^2/\text{hr}$ ) > Area-IV  
 256 ( $1.62 \pm 0.33 \text{ mmol/m}^2/\text{hr}$ ) > Area-III ( $1.46 \pm 0.34 \text{ mmol/m}^2/\text{hr}$ ) (**Fig. 3** and **Fig. 4b**). With the  
 257 exception of March 2019, mean  $\text{CO}_2$  fluxes across the water-air interface show large  
 258 differences among the four water areas ( $p < 0.05$ , **Fig. 4b**).



259

260 Fig. 3. Spatial distribution of CO<sub>2</sub> fluxes across the water-air interface in Wenwusha  
261 Reservoir from November 2018 to June 2019.



262

263 Fig. 4. Variations in mean CO<sub>2</sub> concentrations (a) and fluxes (b) among the four water areas  
264 in Wenwusha Reservoir from November 2018 to June 2019. Different letters denote  
265 significant differences across water areas ( $p < 0.05$ ) based on the results of one-way ANOVA.  
266 Area I, mainly surrounded by urban land ( $n = 28$ ); Area II, mainly surrounded by  
267 agricultural land ( $n = 40$ ); Area III, mainly surrounded by wetland and sporadic agricultural  
268 land ( $n = 12$ ); Area IV, mainly surrounded by forest and sand ( $n = 22$ ). Data were shown with  
269 mean  $\pm$  SE.

### 270 2.3. Spatial variation in CO<sub>2</sub> dynamics between two reservoir areas

271 Significant spatial differences of CO<sub>2</sub> dynamics were also observed between NRA and SRA.  
272 Mean CO<sub>2</sub> concentration and flux in NRA ( $51.32 \pm 3.19$  μmol/L and  $3.72 \pm 0.47$  mmol/m<sup>2</sup>/hr)  
273 were significantly higher than those in SRA ( $29.71 \pm 1.87$  μmol/L and  $1.64 \pm$   
274  $0.22$  mmol/m<sup>2</sup>/hr) ( $p < 0.01$ , Appendix A Fig. S3). Larger CO<sub>2</sub> concentration and emission  
275 were often obtained in the water areas with higher urbanization level around, mainly in NRA  
276 (Fig. 2 and Fig. 3).

## 277 **2.4. Spatial variation in CO<sub>2</sub> dynamics between different microtopographic** 278 **zones**

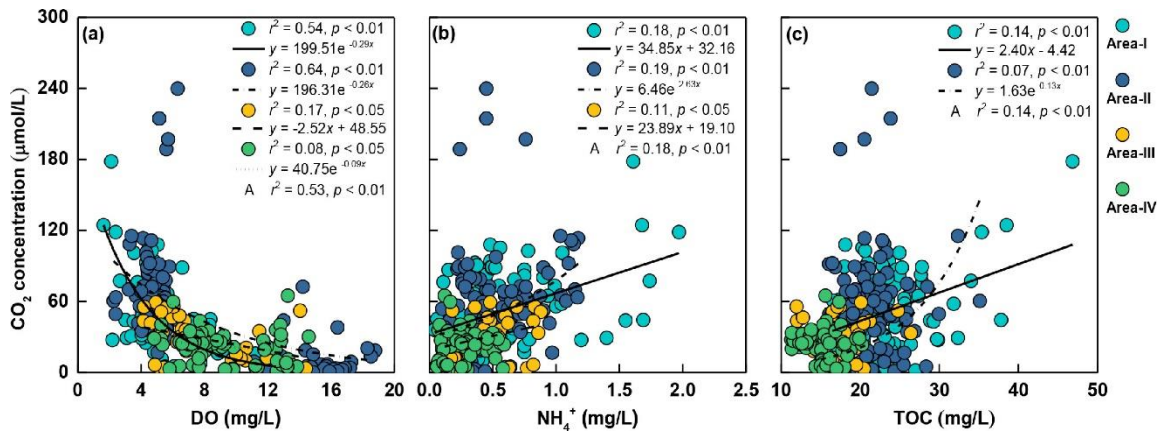
279 CO<sub>2</sub> concentration and flux were compared between different microtopographic zones  
280 (Appendix A **Fig. S4**). The mean dissolved CO<sub>2</sub> concentration in narrow waters ( $52.25 \pm$   
281  $4.62 \mu\text{mol/L}$ ) was significantly higher than that in the open waters ( $37.58 \pm 2.09 \mu\text{mol/L}$ )  
282 ( $p < 0.05$ , Appendix A **Fig. S4a**). No significant difference in mean dissolved  
283 CO<sub>2</sub> concentration was found between the shallow water zone and deep water zone ( $41.51 \pm$   
284  $3.09$  and  $42.09 \pm 2.68 \mu\text{mol/L}$ , respectively,  $p > 0.05$ , Appendix A **Fig. S4b**).  
285 The mean CO<sub>2</sub> fluxes across the water-air interface in the narrow and open waters were  $2.63$   
286  $\pm 0.50 \text{ mmol/m}^2/\text{hr}$  and  $2.83 \pm 0.34 \text{ mmol/m}^2/\text{hr}$ , respectively. The mean CO<sub>2</sub> fluxes in the  
287 shallow water zone and deep water zone were  $2.33 \pm 0.37 \text{ mmol/m}^2/\text{hr}$  and  $3.07 \pm$   
288  $0.40 \text{ mmol/m}^2/\text{hr}$ , respectively (Appendix A **Fig. S4c** and **Fig. S4d**). All sampling sites  
289 showed no significant spatial differences of mean CO<sub>2</sub> flux between different reservoir  
290 microtopographic zones ( $p > 0.05$ , Appendix A **Fig. S4**).

## 291 **2.5. Temporal variation in CO<sub>2</sub> concentration and flux**

292 There were clear seasonal variations in dissolved CO<sub>2</sub> concentration throughout the reservoir  
293 (**Fig. 2**), with the highest concentration in Nov-2018 ( $66.11 \pm 3.97 \mu\text{mol/L}$ ), followed by Jun-  
294 2019 ( $40.77 \pm 2.11 \mu\text{mol/L}$ ) and Mar-2019 ( $18.67 \pm 2.44 \mu\text{mol/L}$ ). CO<sub>2</sub> undersaturation of  
295 water samples (i.e. saturation  $< 100\%$ ) were found in Mar-2019 and Jun-2019 (**Fig. 2**).  
296 There were also seasonal variations in CO<sub>2</sub> fluxes across the water-air interface. CO<sub>2</sub> fluxes  
297 during the whole period ranged from  $-4.09$  to  $33.63 \text{ mmol/m}^2/\text{hr}$ . More than half of the  
298 measurements made in the spring (Mar-2019) exhibited net CO<sub>2</sub> uptake (**Fig. 3**). Seasonal  
299 mean CO<sub>2</sub> fluxes were  $5.19 \pm 0.70 \text{ mmol/m}^2/\text{hr}$  in Nov-2018,  $0.13 \pm 0.15 \text{ mmol/m}^2/\text{hr}$  in Mar-  
300 2019, and  $2.99 \pm 0.29 \text{ mmol/m}^2/\text{hr}$  in Jun-2019, respectively. The four water areas showed  
301 similar seasonal patterns of CO<sub>2</sub> concentrations and fluxes: Mar-2019  $<$  Jun-2019  $<$  Nov-  
302 2018 ( $p < 0.001$ , **Figs. 2–4**).

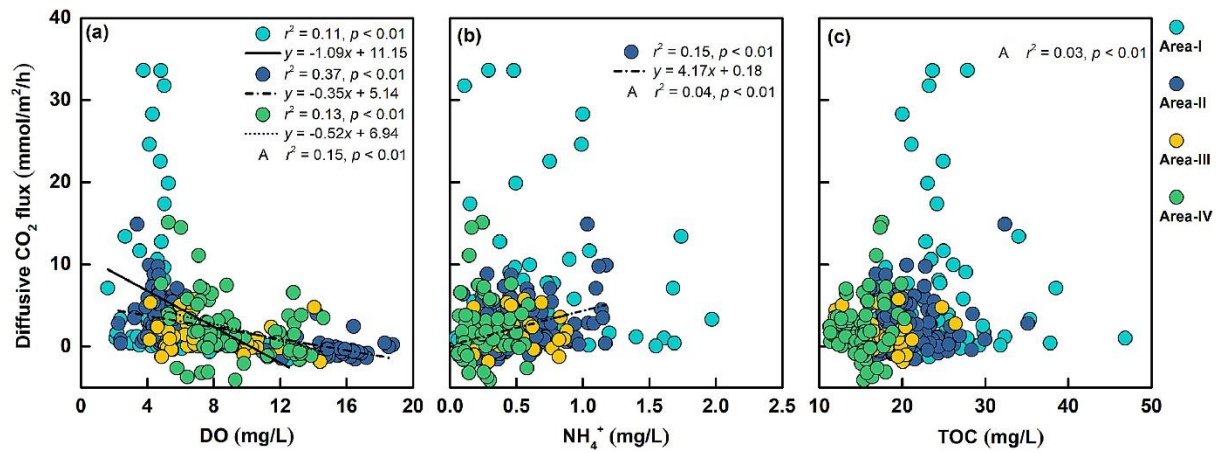
## 303 **2.6. Relationship between CO<sub>2</sub> concentration / flux and water physio-** 304 **chemical properties**

305 Spearman correlations were conducted to examine the relationships between  
306 CO<sub>2</sub> concentration (or flux) with the physio-chemical properties of water  
307 (**Fig. 5, 6** and **Table 3**). Dissolved CO<sub>2</sub> concentrations were positively correlated with pH,  
308 NH<sub>4</sub><sup>+</sup>, TDN and TOC, but negatively correlated with water temperature and DO  
309 ( $p < 0.01$ , **Table 3**). CO<sub>2</sub> fluxes were positively correlated with TOC and NH<sub>4</sub><sup>+</sup>, but negatively  
310 correlated with DO ( $p < 0.05$ , **Table 3**). Notably, the significance and strength of correlations  
311 were different among four water areas. CO<sub>2</sub> concentrations and fluxes were significantly and  
312 negatively correlated with DO concentrations in three water areas except Area-III  
313 (**Fig. 5a** and **6a**). CO<sub>2</sub> concentrations were positively correlated with NH<sub>4</sub><sup>+</sup> and TOC  
314 concentrations, with stronger relationships found in Area-I and Area-II (**Fig. 5b** and **5c**).



315

316 Fig. 5. Relationships of CO<sub>2</sub> concentration against DO (a), NH<sub>4</sub><sup>+</sup> (b), and TOC (c) in the four  
 317 water areas. Letter A in the legend denotes all water areas combined.



318

319 Fig. 6. Relationships of CO<sub>2</sub> flux against DO (a), NH<sub>4</sub><sup>+</sup> (b), and TOC (c) in the four water  
 320 areas. Letter A in the legend denotes all water areas combined.

321

322

323 **Table 3**

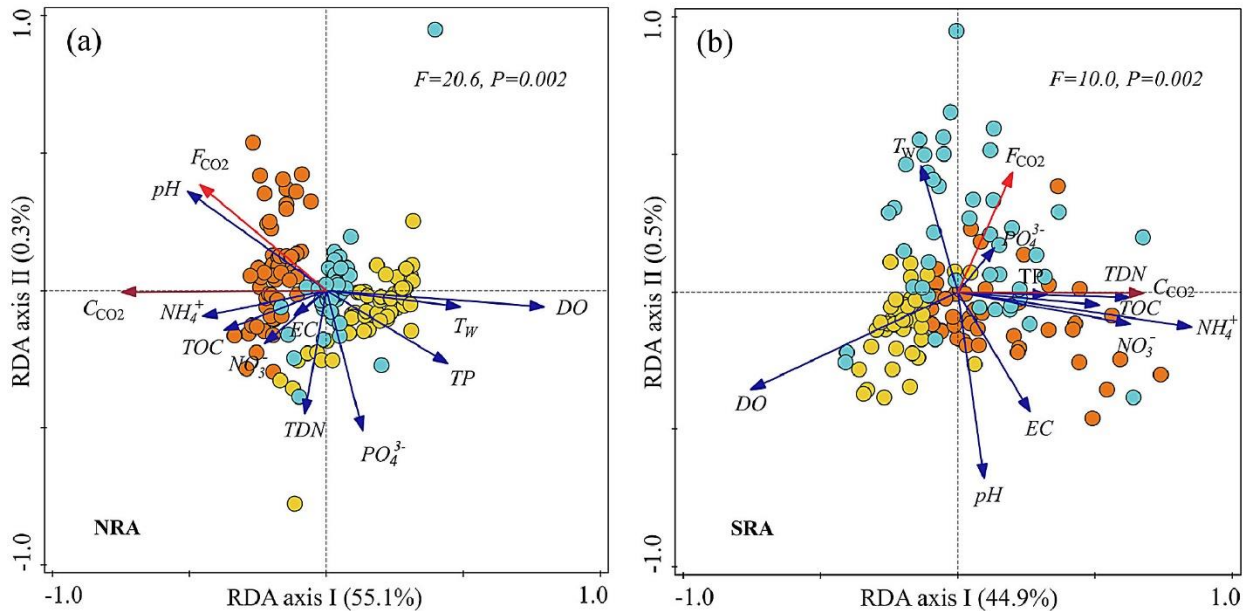
324 Spearman correlation coefficients of CO<sub>2</sub> concentration (flux) with environmental variables in the  
325 whole Wenwusha Reservoir during the research period.

Environmental variables	CO <sub>2</sub> concentration	CO <sub>2</sub> flux
Water temperature (Tw)	-0.226**	NS
pH	0.195**	NS
Dissolved oxygen (DO)	-0.732**	-0.573**
Total organic carbon (TOC)	0.381**	0.137*
Ammonia (NH <sub>4</sub> <sup>+</sup> )	0.471**	0.323**
Total dissolved nitrogen (TDN)	0.151**	NS
Phosphate (PO <sub>4</sub> <sup>3-</sup> )	NS	NS

326 NS means “nonsignificant correlation”. Symbols \* and \*\* indicate significant correlations at 0.05 and 0.01 levels,  
327 respectively.

328

329 Redundancy analysis (RDA) was performed for the two reservoir areas, NRA and SRA, with  
 330 CO<sub>2</sub> concentration and flux as the response variables and water physio-chemical properties as  
 331 the explanatory variables. In NRA, axis I explained 55.1% of the variations in  
 332 CO<sub>2</sub> concentration and flux, with DO and TOC being the most powerful predictors (**Fig. 7**).  
 333 In SRA, axis I explained 44.9% of the variations in CO<sub>2</sub> concentration and flux, with NH<sub>4</sub><sup>+</sup>,  
 334 DO, and TOC being the major controlling factors (**Fig. 7**).



335 ● Nov-2018 ● Mar-2019 ● Jun-2019  
 336 Fig. 7. Results of redundancy analysis (RDA) showing the relations between  
 337 CO<sub>2</sub> concentration (or CO<sub>2</sub> flux) and water physico-chemical properties including *T<sub>w</sub>* (water  
 338 temperature), pH, *EC* (conductivity), *DO* (dissolved oxygen), NO<sub>3</sub><sup>-</sup> (nitrate nitrogen),  
 339 NH<sub>4</sub><sup>+</sup> (ammonia nitrogen), PO<sub>4</sub><sup>3-</sup> (phosphate), and *TP* (total phosphorus), in the north  
 340 reservoir area (NRA) (a) and the south reservoir area (SRA) (b) in Wenwusha Reservoir.

### 341 3. Discussion

#### 342 3.1. Effects of watershed urbanization and land use types on CO<sub>2</sub> dynamics

343 Land use change in the catchment can disturb the biogeochemical cycling on land and in  
 344 adjacent waters (Lai et al., 2016; Zhang et al., 2015), resulting in large spatial variations in  
 345 CO<sub>2</sub> fluxes (Kamjunke et al., 2013; Pacheco et al., 2015). In our study, the concentrations of  
 346 carbon and nitrogen substrates (TOC, NH<sub>4</sub><sup>+</sup> and TDN) in Area-III and Area-IV were  
 347 substantially lower than those in Area-I and Area-II where waters were close to municipal  
 348 and agricultural lands (**Table 2** and Appendix A **Fig. S3**). The CO<sub>2</sub> concentrations and fluxes  
 349 increased with TOC and NH<sub>4</sub><sup>+</sup> concentrations across the whole reservoir ( $p < 0.05$ , **Table 3**).  
 350 Our results revealed that the spatial variation in CO<sub>2</sub> flux in the subtropical Wenwusha  
 351 reservoir was affected by anthropogenic activities (e.g., urbanization and land use change) in  
 352 the catchment, which were similar to previous findings (Marescaux et al., 2018; Wang et al.,  
 353 2017) that CO<sub>2</sub> production and emission in the waters increased with the levels of  
 354 urbanization and sewage discharge. Two underlying processes may account for this: (1) the  
 355 large TOC load from municipal and aquaculture effluents provides more substrates for *in*  
 356 *situ* heterotrophic respiration (Almeida et al., 2016; Crawford et al., 2013); (2) additional  
 357 nitrogen loading in water areas with high organic carbon concentrations (e.g. Area I) can

358 ameliorate nitrogen limitation on microbial decomposition and promote net CO<sub>2</sub> production  
359 (Bodmer et al., 2016; Marescaux et al., 2018;).

360 The highest mean CO<sub>2</sub> flux observed in Area-I provided additional evidence for the impact of  
361 urbanization on CO<sub>2</sub> emission from our reservoir. In general, urban and agricultural sewage  
362 carries abundant dissolved CO<sub>2</sub> (Webb et al., 2016; Yang et al., 2018; Yu et al., 2017). The  
363 spatial variation in reservoir CO<sub>2</sub> flux adjacent to urban areas is thus often affected by sewage  
364 discharge. In this study, we observed that the dissolved CO<sub>2</sub> concentrations in the sewage  
365 drainage channels, aquaculture ponds, and rivers adjacent to the reservoir were about three  
366 times higher than those in the reservoir surface water. This resulted in the direct input of  
367 dissolved CO<sub>2</sub> into the Wenwusha Reservoir, and subsequently a larger CO<sub>2</sub> diffusive flux  
368 because of the steeper CO<sub>2</sub> concentration gradient between the surface water and the  
369 atmosphere. Therefore, the discharge of CO<sub>2</sub>-rich wastewater can directly contribute to  
370 CO<sub>2</sub> oversaturation in some polluted waters and lead to high CO<sub>2</sub> emissions from reservoir  
371 water to the atmosphere (Li et al., 2020a; 2020b).

372 Topography can also influence the transport and distribution of pollutants. Pollutants tend to  
373 accumulate in the narrow coastal waters due to their low water exchange and dilution effect  
374 (e.g. Arneeth et al., 2017; Li et al., 2013; Ni et al., 2019). For instance, Natchimuthu et al.  
375 (2017) reported that small and narrow lakes had higher *p*CO<sub>2</sub> and CO<sub>2</sub> fluxes in a Swedish  
376 catchment. Similar observations have been found in other aquatic ecosystems with  
377 varying microtopography (Raymond and Cole, 2003; Schilder et al., 2013; Wang et al.,  
378 2017). Across the entire Wenwusha Reservoir, the mean CO<sub>2</sub> concentrations and fluxes from  
379 the shallow water zone to deep water zone showed no significant difference ( $p > 0.05$ ,  
380 Appendix A **Fig S4c** and **S4d**). The reservoir was shallow, with mean and maximum depths  
381 of 1.5 and 4.0 m, respectively. The reservoir bottom was quite flat with little variations in  
382 sediment-to-water volume ratio among reservoir areas (Gruber et al., 2019; Roland et al.,  
383 2010; Wilson et al., 2015), which resulted in limited effects of depth on DOC concentration  
384 and sediment respiration. Moreover, CO<sub>2</sub> concentrations increased significantly from the  
385 open water areas to the narrow areas ( $p < 0.05$ , Appendix A **Fig S4a**), which might be related  
386 to the coupling of high pollution load and topography (Kortelainen et al., 2006; Roland et al.,  
387 2010; Zhang et al., 2019). On one hand, narrow waters have relatively lower velocity and a  
388 more enclosed environment than other parts of the reservoir (Holgerson, 2015; Xiao et al.,  
389 2017), providing favorable conditions for the accumulation of fresh sediments and thus  
390 respiratory CO<sub>2</sub> production. On the other hand, the narrow waters adjacent to aquaculture  
391 ponds and ditches can receive abundant non-point source sewage. Similar to the spatial  
392 patterns of CO<sub>2</sub> concentration, TOC, NH<sub>4</sub><sup>+</sup>, and TDN concentrations at the narrow waters  
393 were approximately 28%, 100%, and 27% larger than those at the open areas, which  
394 supported the above hypothesis.

### 395 **3.2. Temporal variation in CO<sub>2</sub> emission**

396 During the study period, mean CO<sub>2</sub> concentrations in Wenwusha Reservoir exhibited  
397 prominent seasonal fluctuations with higher value in autumn (Nov-2018) and lower value in  
398 spring (Mar-2019) (**Fig. 4a**). Correspondingly, CO<sub>2</sub> flux followed the same temporal pattern  
399 (**Fig. 4b**). In general, net CO<sub>2</sub> flux (release / uptake) in aquatic ecosystems reflects the  
400 balance between CO<sub>2</sub> production and consumption (Jonsson et al., 2003; Bellido et al.,  
401 2009; Pacheco et al., 2015). Some researches attributed the variability of CO<sub>2</sub> flux to organic  
402 matter decomposition (Wang et al., 2017), primary productivity (Sobek et al., 2005), and  
403 meteorological conditions (Butman and Raymond, 2011; Natchimuthu et al., 2014).

404 Biodegradation of organic carbon is regarded as an important source of CO<sub>2</sub> production  
405 (Barros et al., 2011; Crawford et al., 2013; Demarty et al., 2009). However, our

406 measurements showed no significant seasonal change in TOC (**Table 2**), which was different  
407 from the temporal patterns of CO<sub>2</sub> concentrations and fluxes in the reservoir. Therefore,  
408 substrate supply was likely not a key factor affecting the temporal dynamics of CO<sub>2</sub> in  
409 Wenwusha Reservoir. Algal photosynthesis consumes CO<sub>2</sub>, which can play an important role  
410 in governing the temporal variation in CO<sub>2</sub> flux (Kutzbach et al., 2007; Scofield et al.,  
411 2016; Yao et al., 2007). Chl-*a* is an important parameter characterizing algal primary  
412 production. Despite the lack of significant correlation observed between Chl-*a* and CO<sub>2</sub> flux  
413 in the current research, the seasonal pattern of mean water Chl-*a* concentration was opposite  
414 to that of CO<sub>2</sub> (**Fig. 4** and Appendix A **Fig. S5**). Limited by the low temperature, relatively  
415 lower Chl-*a* concentration and the highest CO<sub>2</sub> emissions were seen in November 2018.  
416 Higher Chl-*a* concentration coincided with rising temperature in spring, accounting for the  
417 lower CO<sub>2</sub> concentration and flux in March 2019 (Appendix A **Fig. S5**). It should be noted  
418 that precipitation and its dilution effect on Chl-*a* in water could also influence the seasonal  
419 variation in CO<sub>2</sub> flux (Holgerson, 2015; Zhang et al., 2019). In addition, on rainy days,  
420 photosynthesis could be constrained by lower solar radiation. Frequent rainfall events  
421 between April and June 2019 (total precipitation of 625.6 mm) (Appendix A **Fig. S1**) reduced  
422 Chl-*a* concentration in the reservoir to some extent. Thus, the higher CO<sub>2</sub> flux detected in  
423 summer (June-2019) than in spring (Mar-2019) was probably in part due to the greater  
424 number of rainy days and the subsequent decline of sunlight-driven photosynthesis. In the  
425 subtropical coastal reservoir, therefore, our findings demonstrated that primary productivity  
426 could exert an impact on the seasonal variation in CO<sub>2</sub> fluxes between seasons, which in turn  
427 would be related to precipitation and temperature.

### 428 **3.3. CO<sub>2</sub> fluxes in comparison with previous estimates**

429 The average CO<sub>2</sub> flux from Wenwusha Reservoir was  $2.77 \pm 0.28$  mmol/m<sup>2</sup>/h, which was  
430 lower than those reported in some tropical waters (e.g. Abril et al., 2005; Dos Santos et al.,  
431 2006; Guérin et al., 2006) (**Table 4**). However, we noticed that the CO<sub>2</sub> fluxes from our  
432 reservoir were markedly higher than those in most temperate and subtropical reservoirs  
433 worldwide, such as Lake Lynch in Chile (Gerardo-Nieto et al., 2017), Eagle Creek reservoir  
434 in the USA (Jacinthe et al., 2012), cascade reservoirs on Maotiao river in China (Wang et al.,  
435 2011), and Danjiangkou reservoir in China (Li and Zhang, 2014) (**Table 4**). Our results of  
436 flux upscaling to the whole-reservoir scale based on our high spatial resolution data showed  
437 that Wenwusha reservoir emitted approximately 3.91 Gg CO<sub>2</sub> per year. The total CO<sub>2</sub> flux  
438 from Wenwusha reservoir would hence account for approximately 0.0241% of the annual  
439 total from all the reservoirs in China (Li et al., 2018). The results of this study showed that  
440 the subtropical coastal reservoir such as Wenwusha reservoir could be potential sources of  
441 atmospheric CO<sub>2</sub> and therefore would deserve more attention.

442

443 **Table 4**444 Ranges of CO<sub>2</sub> fluxes (mmol m<sup>-2</sup> h<sup>-1</sup>) from different types of reservoirs in the world.

Climate	Site	Main land use in the catchment	$F_{CO_2}$ (mmol m <sup>-2</sup> h <sup>-1</sup> )	Reference
Temperate	Lake Lynch, Chile	Forest	0.49 – 0.57 (0.52)	Gerardo-Nieto et al., 2017
	L.Skinnmuddselet, Sweden	Forest, mire	----- (0.83)	Áberg et al., 2004
	Porttipahta, Finland	Forest, pond	0.83 – 2.17 (1.46)	Huttunen et al., 2003
	Lokka, Finland	Peatland	0.46 – 3.04 (1.44)	Huttunen et al., 2003
	Eagle Creek, USA	Agriculture, grassland, forest	-1.28 – 15.10 (1.90)	Jacinthe et al., 2012
Subtropical	Danjiangkou, China	Forest, grassland, farmland	-0.34 – 1.31 (0.38)	Li & Zhang, 2014
	Xiuwen, China	-----	-0.25 – 3.71 (1.96)	Wang et al., 2011
	Chongqing, China	Urban	-0.42 – 21.25 (5.73)	Wang et al., 2017
	Chongqing, China	Agriculture	-0.48 – 7.20 (2.01)	Wang et al., 2017
	Al-Wihdeh, King Talal, Wadi , Al-Arab, Jordan	-----	-1.10 – 16.52 (3.12)	Alshboul et al., 2015
	Wenwusha, China	Urban, agriculture, forest, wetland	-4.09 – 33.63 (2.77)	This study
Tropical	Petit Saut, French Guiana	Tropical forest	-0.42 – 15.42 (5.54)	Abril et al., 2005
	Tucurui, Brazil	Tropical forest	----- (7.92)	Dos Santos et al., 2006
	Samuel, Balbina, Brazil	Tropical forest	10.58 – 16.33	Guerin et al., 2006
	Cerrado, Brazil	-----	-0.34 – 16.62	Roland et al., 2011
-----	China's reservoirs	-----	----- (1.85)	Li et al., 2018
	Global reservoirs	-----	----- (1.14)	Deemer et al., 2016

445 Figures in brackets are averages. “-----” means no data.

446 Notably, the average CO<sub>2</sub> flux in waters adjacent to the urban area (Area-I,  $5.05 \pm$   
447  $0.87 \text{ mmol/m}^2/\text{hr}$ ) was 1.72 – 3.46 times of that in other water areas in Wenwusha Reservoir  
448 (**Fig. 3** and **Fig. 4b**). Moreover, the mean CO<sub>2</sub> flux in Area-I was close to the level seen in  
449 some tropical reservoirs (Barros et al., 2011) and urban reservoirs in Chongqing, Southwest  
450 China ( $5.73 \pm 3.38 \text{ mmol/m}^2/\text{hr}$ ) (Wang et al., 2017), where urban pollution was the major  
451 contributor to CO<sub>2</sub> production. In contrast with the findings from several reservoirs in  
452 Chongqing (Wang et al., 2017), our results showed that the influence of urbanization on  
453 CO<sub>2</sub> emission from adjacent waters could also exist in different areas within a single reservoir  
454 ecosystem. These results together indicated the crucial role of urbanization in carbon  
455 biogeochemical cycling in reservoir waters.

### 456 **3.4. Uncertainties and further outlook**

457 There are several limitations in our study that are worthy addressing. Firstly, our results have  
458 shown large spatiotemporal variations in CO<sub>2</sub> concentration and flux in the reservoir. In  
459 future studies, field sampling with a greater frequency over multiple years can provide more  
460 detailed information about the temporal variations in CO<sub>2</sub> dynamics at multiple scales.  
461 Secondly, the diel fluctuations of GHG flux have been reported in various aquatic ecosystems  
462 (Natchimuthu et al., 2014; Xiao et al., 2013; Xing et al., 2004). Photosynthesis is typically  
463 strong during the day, while respiration dominates CO<sub>2</sub> exchange with markedly higher  
464 CO<sub>2</sub> emission at night (Hirota et al., 2007). Therefore, aquatic ecosystems can be a net carbon  
465 sink during the daytime due to the strong phytoplankton photosynthesis, but change to a net  
466 carbon source when considering a complete 24-hour cycle owing to the strong carbon  
467 emission at night (Natchimuthu et al., 2014). Similar diel patterns can also occur in the  
468 reservoir on top of the seasonal variation. A greater number of *in situ* measurement of the  
469 diurnal CO<sub>2</sub> fluxes in different seasons will further improve our development of annual  
470 CO<sub>2</sub> budgets in the aquatic ecosystems. Furthermore, some studies have shown the important  
471 role of meteorological variables in affecting CO<sub>2</sub> emission (Li and  
472 Lu, 2012; Natchimuthu et al., 2014; Zhao et al., 2013). Although the effect of extreme  
473 weather events, such as heavy rain and typhoon, on CO<sub>2</sub> flux was not examined in this study,  
474 we found some clear impacts of continuous precipitation on reservoir CO<sub>2</sub> fluxes. The  
475 impacts of meteorological events deserve more attention in future studies. Due to the  
476 limitation of equipment, we did not measure sewage discharge and nutrient concentrations in  
477 this study. In future work, quantifying the rates of water and nutrient inputs from sewage can  
478 provide useful information to improve the understanding of the impact of urbanization and  
479 land use on carbon cycling in reservoirs. Lastly, we focused our investigation of the controls  
480 of CO<sub>2</sub> concentration and flux on various environmental parameters (e.g. water quality,  
481 weather condition, and reservoir morphology). Future research can quantify the  
482 biogeochemical processes of CO<sub>2</sub> using molecular biotechnology and isotope methods to  
483 yield a better mechanistic understanding of the spatiotemporal dynamics of CO<sub>2</sub> in aquatic  
484 ecosystems.

### 485 **4. Conclusions**

486 With the worsening climate change, GHG emission from reservoirs have received increasing  
487 attention. In this study, dissolved CO<sub>2</sub> concentration and flux were investigated at high spatial  
488 resolution from a subtropical coastal Wenwusha Reservoir, Southeast China. Overall, our  
489 results showed that CO<sub>2</sub> concentrations in the reservoir were supersaturated (average:  
490  $24.25 \text{ mol/m}^2/\text{y}$ ) in most periods, varying over a wide range from  $-35.82$  to  $294.60 \text{ mol/m}^2/\text{y}$ .  
491 CO<sub>2</sub> concentrations and fluxes from waters adjacent to regions with intensive human activity  
492 were much higher than those in other areas, due to larger input of allochthonous carbon and  
493 nitrogen via municipal sewage, aquaculture wastewater and upstream runoff. Urbanization

494 and agricultural activities in the catchment appeared to create CO<sub>2</sub> emission hotspots in some  
495 parts of the reservoir. Apart from the spatial differences across the reservoir, reservoir  
496 CO<sub>2</sub> emissions also exhibited clear seasonal variations that were related to primary  
497 productivity, temperature, and rainfall events. Our results highlighted that subtropical coastal  
498 reservoir was a net source of atmospheric CO<sub>2</sub> with high spatiotemporal heterogeneity.  
499 Considering the rapid urbanization in coastal areas around the world, proactive measures are  
500 needed to mitigate the large GHG emission from coastal reservoirs arising from human  
501 activities.

## 502 **Acknowledgment**

503 This research was supported by the National Science Foundation of  
504 China (Nos. 41801070, 41671088), the National Science Foundation of  
505 Fujian Province (No. 2020J01136), 2020 Innovation Training Programme Project for Fujian  
506 Normal University Student's (No. cxxl-2020270), the Research Grants Council of the Hong  
507 Kong Special Administrative Region, China (Nos. CUHK458913, 14302014, 14305515),  
508 the CUHK Direct Grant (No. SS15481), Open Research Fund Program of Jiangsu Key  
509 Laboratory of Atmospheric Environment Monitoring and Pollution Control (No. KHK1806),  
510 a project funded by the Priority Academic Program Development of Jiangsu Higher  
511 Education Institutions (PAPD) and the Minjiang Scholar Programme.

## 512 **References**

- 513 Åberg, J., Bergström, A.K., Algesten, G., Söderback, K., Jansson, M., 2004. A comparison of  
514 the carbon balances of a natural lake (L.Örträsket) and a hydroelectric reservoir  
515 (L.Skinnmuddselet) in northern Sweden. *Water Res.* 38, 531–538. <https://doi.org/10.1016/j.watres.2003.10.035>.
- 517 Abril, G., Guerin, F., Richard, S., Delmas, R., Galy-Lacaux, C., Gosse, P., Tremblay, A.,  
518 Varfalvy, L., Dos Santos, M.A., Matvienko, B., 2005. Carbon dioxide and methane  
519 emissions and the carbon budget of a 10-year old tropical reservoir (Petit Saut, French  
520 Guiana). *Glob. Biogeochem. Cycles* 19. <https://doi.org/10.1029/2005GB002457>.
- 521 Almeida, R.M., Paranaíba J.R., Barbosa Í., Sobek S., Kosten S., Linkhorst A., Mendonça R.,  
522 Quadra G., Roland F., Barros N., 2019. Carbon dioxide emission from drawdown areas of  
523 a Brazilian reservoir is linked to surrounding land cover. *Aquatic. Ecos. Syst.* 81, 1–9.  
524 <https://doi.org/10.1007/s00027-019-0665-9>.
- 525 Almeida, R.M., Nóbrega, G.N., Junger, P.C., Figueiredo, A.V., Andrade, A.S., de Moura,  
526 C.G.B., Tonetta, D., Oliveira, E.S., Araújo, F., Rust, F., Piñeiro-Guerra, J.M., Mendonça,  
527 J.R., Medeiros, L.R., Pinheiro, L., Miranda, M., Costa, M.R.A., Melo, M.L., Nobre,  
528 R.L.G., Benevides, T., Roland, F., De Klein, J., Barros, N.O., Mendonça, R., Becker, V.,  
529 Huszar, V.L.M., Kosten, S., 2016. High primary production contrasts with intense carbon  
530 emission in a eutrophic tropical reservoir. *Front. Microbiol.* 7, 717. <https://doi.org/10.3389/fmicb.2016.00717>.
- 532 Alshboul, Z., Lorke, A., 2015. Carbon dioxide emissions from reservoirs in the lower Jordan  
533 watershed. *Plos One* 10. <https://doi.org/10.1371/journal.pone.0143381>.
- 534 Arneeth, A., Sitch, S., Pongratz, J., Stocker, B.D., Ciais, P., Poulter, B., Bayer, A.D., Bondeau,  
535 A., Calle, L., Chini, L.P., Gasser, T., Fader, M., Friedlingstein, P., Kato, E., Li, W.,  
536 Lindeskog, M., Nabel, J.E.M.S., Pugh, T.A.M., Robertson, E., Viogy, N., Yue, C.,  
537 Zaehle, S., 2017. Historical carbon dioxide emissions caused by land-use changes are  
538 possibly larger than assumed. *Nat. Geosci.* 10, 79. <https://doi.org/10.1038/ngeo2882>.

539 Barros, N., Cole, J.J., Tranvik, L.J., Prairie, Y.T., Bastviken, D., Huszar, V.L.M., Del  
540 Giorgio, P., Roland, F., 2011. Carbon emission from hydroelectric reservoirs linked to  
541 reservoir age and latitude. *Nat. Geosci.* 4, 593–596. <https://doi.org/10.1038/ngeo1211>.

542 Bellido, J.L., Tulonen, T., Kankaala, P., Ojala, A., 2009. CO<sub>2</sub> and CH<sub>4</sub> fluxes during spring  
543 and autumn mixing periods in a boreal lake (paajarvi, southern finland). *J. Geophys. Res-*  
544 *Biogeosci.* 114. <https://doi.org/10.1029/2009jg000923>.

545 Bevelhimer, M.S., Stewart, A.J., Fortner, A.M., Phillips, J.R., Mosher, J.J., 2016. CO<sub>2</sub> is  
546 dominant greenhouse gas emitted from six hydropower reservoirs in southeastern United  
547 States during peak summer emissions. *Water* 8, 1–14. <http://doi.org/10.3390/w8010015>.

548 Bodmer, P., Heinz, M., Pusch, M., Singer, G., Premke, K., 2016. Carbon dynamics and their  
549 link to dissolved organic matter quality across contrasting stream ecosystems. *Sci. Total*  
550 *Environ.* 553, 574–586. <http://doi.org/10.1016/j.scitotenv.2016.02.095>.

551 Butman, D., Raymond, P.A., 2011. Significant efflux of carbon dioxide from streams and  
552 rivers in the united states. *Nat. Geosci.* 4, 839–842. <http://doi.org/10.1038/ngeo1294>.

553 Chao, B.F., Wu, Y.H., Li, Y.S., 2008. Impact of artificial reservoir water impoundment on  
554 global sea level. *Science* 320, 212–214. <http://doi.org/10.1126/science.1154580>.

555 Cole, J.J., Bade, D.L., Bastviken, D., Pace, M.L., Van De Bogert, M., 2010. Multiple  
556 approaches to estimating air-water gas exchange in small lakes. *Limnol. Oceanogr-Meth.*  
557 8, 285–293. <http://doi.org/10.4319/lom.2010.8.285>.

558 Crawford, J.T., Striegl, R.G., Wickland, K.P., Dornblaser, M.M., Stanley, E.H., 2013.  
559 Emissions of carbon dioxide and methane from a headwater stream network of interior  
560 alaska. *J. Geophys. Res-Biogeosci.* 118, 482–494. <http://doi.org/10.1002/jgrg.20034>.

561 Crusius, J., Wanninkhof, R., 2003. Gas transfer velocities measured at low wind speed over a  
562 lake. *Limnol. Oceanogr.* 48, 1010–1017. <http://doi.org/10.4319/lo.2003.48.3.1010>.

563 Deemer, B.R., Harrison, J.A., Li, S.Y., Beaulieu, J.J., Delsonro, T., Barros, N., Bezerra-  
564 Neto, J.F., Powers, S.M., Santos, M.A.D., Vonk, J.A., 2016. Greenhouse gas emissions  
565 from reservoir water surfaces: a new global synthesis. *Bioscience* 66, 949–964.  
566 <https://doi.org/10.1093/biosci/biw117>.

567 Demarty, M., Bastien, J., Tremblay, A., Hesslein, R.H., Gill, R., 2009. Greenhouse gas  
568 emissions from boreal reservoirs in manitoba and quebec, canada, measured with  
569 automated systems. *Environ. Sci. Technol.* 43, 8908–8915. [http://doi.org/10.1021/](http://doi.org/10.1021/es8035658)  
570 [es8035658](http://doi.org/10.1021/es8035658).

571 De Mello, K., Valente, R.A., Randhir, T.O., Alves Dos Santos, A.C., Vettorazzi, C.A., 2018.  
572 Effects of land use and land cover on water quality of low-order streams in southeastern  
573 brazil: Watershed versus riparian zone. *Catena* 167, 130–138. [http://doi.org/](http://doi.org/10.1016/j.catena.2018.04.027)  
574 [10.1016/j.catena.2018.04.027](http://doi.org/10.1016/j.catena.2018.04.027).

575 Dodds, W.K., Cole, J.J., 2007. Expanding the concept of trophic state in aquatic ecosystems:  
576 It's not just the autotrophs. *Aquat. Sci.* 69, 427–439. [http://doi.org/10.1007/s00027-007-](http://doi.org/10.1007/s00027-007-0922-1)  
577 [0922-1](http://doi.org/10.1007/s00027-007-0922-1).

578 Dos Santos, M.A., Rosa, L.P., Sikar, B., Sikar, E., Dos Santos, E.O., 2006. Gross greenhouse  
579 gas fluxes from hydro-power reservoir compared to thermo-power plants. *Energ. Policy*  
580 34, 481–488. <http://doi.org/10.1016/j.enpol.2004.06.015>.

581 Domingues R.B., Catia G.C., Galvao H.M., Brotas V., Barbosa A.B., 2016. Short-term  
582 interactive effects of ultraviolet radiation, carbon dioxide and nutrient enrichment on

583 phytoplankton in a shallow coastal lagoon. *Aquat. Ecol.* 51, 91–105.  
584 <http://doi.org/10.1007/s10452-016-9601-4>.

585 Fearnside P.M., 2005. Brazil's Samuel dam: Lessons for hydroelectric development policy  
586 and the environment in Amazonia. *Environ. Manage.* 2005, 399, 1–19. [http://doi.org/](http://doi.org/10.1007/s00267-004-0100-3)  
587 [10.1007/s00267-004-0100-3](http://doi.org/10.1007/s00267-004-0100-3).

588 Fuzhou Municipal Water Authorities, 2019. *Water Resources Bulletin* in 2018.  
589 [http://slj.fuzhou.gov.cn/zz/zyxz/201912/t20191205\\_3109364.htm.pdf](http://slj.fuzhou.gov.cn/zz/zyxz/201912/t20191205_3109364.htm.pdf) (In Chinese).

590 Gerardo-Nieto, O., Soledad Astorga-Espana, M., Mansilla, A., Thalasso, F., 2017. Initial  
591 report on methane and carbon dioxide emission dynamics from sub-antarctic freshwater  
592 ecosystems: A seasonal study of a lake and a reservoir. *Sci. Total Environ.* 593, 144–154.  
593 <http://doi.org/10.1016/j.scitotenv.2017.02.144>.

594 Gruber, N., Clement, D., Carter, B.R., Feely, R.A., Van Heuven, S., Hoppema, M., Ishii, M.,  
595 Key, R.M., Kozyr, A., Lauvset, S.K., Lo Monaco, C., Mathis, J.T., Murata, A., Olsen, A.,  
596 Perez, F.F., Sabine, C.L., Tanhua, T., Wanninkhof, R., 2019. The oceanic sink for  
597 anthropogenic CO<sub>2</sub> from 1994 to 2007. *Science* 363, 1193. [http://doi.org/](http://doi.org/10.1126/science.aau5153)  
598 [10.1126/science.aau5153](http://doi.org/10.1126/science.aau5153).

599 Guérin, F., Abril, G., Richard, S., Burban, B., Reynouard, C., Seyler, P., Delmas, R., 2006.  
600 Methane and carbon dioxide emissions from tropical reservoirs: significance of  
601 downstream rivers. *Geophys. Res. Lett.* 33, L21407. [http://doi.org/10.1029/](http://doi.org/10.1029/2006GL027929)  
602 [2006GL027929](http://doi.org/10.1029/2006GL027929).

603 Guérin, F., Abril, G., Serca, D., Delon, C., Richard, S., Delmas, R., Tremblay, A., Varfalvy,  
604 L., 2007. Gas transfer velocities of CO<sub>2</sub> and CH<sub>4</sub> in a tropical reservoir and its river  
605 downstream. *J. Mar. Syst.* 66, 161–172. <https://doi.org/10.1016/j.jmarsys.2006.03.019>.

606 Hao, B.F., Ma, M.G., Li, S.W., Li, Q.P., Hao, D.L., Huang, J., Ge, Z.X., Yang, H., Han, X.J.,  
607 2019. Land Use Change and Climate Variation in the Three Gorges Reservoir Catchment  
608 from 2000 to 2015 Based on the Google Earth Engine. *Sensors* 19(9). [https://doi.org/](https://doi.org/10.3390/s19092118)  
609 [10.3390/s19092118](https://doi.org/10.3390/s19092118).

610 Hertwich, E.G., 2013. Addressing biogenic greenhouse gas emissions from hydropower in  
611 LCA. *Environ. Sci. Technol.* 47, 9604–9611. <https://doi.org/10.1021/es401820p>.

612 Hirota, M., Senga, Y., Seike, Y., Nohara, S., Kunii, H., 2007. Fluxes of carbon dioxide,  
613 methane and nitrous oxide in two contrastive fringing zones of coastal lagoon, Lake  
614 Nakaumi, Japan. *Chemosphere* 68, 597–603. [https://doi.org/10.1016/j.chemosphere.](https://doi.org/10.1016/j.chemosphere.2007.01.002)  
615 [2007.01.002](https://doi.org/10.1016/j.chemosphere.2007.01.002).

616 Hodson, A., Nowak, A., Holmlund, E.S., Redeker, K.R., Christiansen, H.H., 2019. Seasonal  
617 Dynamics of Methane and Carbon Dioxide Evasion From an Open System Pingo: Lagoon  
618 Pingo, Svalbard. *Front. Earth Sci.* 7, 30. <https://doi.org/10.3389/feart.2019.00030>.

619 Hu, B.B., Wang, D.Q., Zhou, J., Meng, W.Q., Li, C.W., Sun, Z.B., Guo, X., Wang, Z.L.,  
620 2018. Greenhouse gases emission from the sewage draining rivers. *Sci. Total Environ.*  
621 612, 1454–1462. <https://doi.org/10.1016/j.scitotenv.2017.08.055>.

622 Huttunen, J.T., Vaisanen, T.S., Hellsten, S.K., Heikkinen, M., Nykanen, H., Jungner, H.,  
623 Niskanen, A., Virtanen, M.O., Lindqvist, O.V., Nenonen, O.S., Martikainen, P.J., 2002.  
624 Fluxes of CH<sub>4</sub>, CO<sub>2</sub>, and N<sub>2</sub>O in hydroelectric reservoirs Lokka and Porttipahta in the  
625 northern boreal zone in Finland. *Glob. Biogeochem. Cy.* 16, 1003. [https://doi.org/](https://doi.org/10.1029/2000GB001316)  
626 [10.1029/2000GB001316](https://doi.org/10.1029/2000GB001316).

- 627 Holgerson, M.A., 2015. Drivers of carbon dioxide and methane supersaturation in small,  
628 temporary ponds. *Biogeochemistry* 124, 305–318. [https://doi.org/10.1007/s10533-015-](https://doi.org/10.1007/s10533-015-0099-y)  
629 [0099-y](https://doi.org/10.1007/s10533-015-0099-y).
- 630 Jacinthe, P.A., Filippelli, G.M., Tedesco, L.P., Raftis, R., 2012. Carbon storage and  
631 greenhouse gases emission from a fluvial reservoir in an agricultural landscape. *Catena*  
632 94, 53–63. <https://doi.org/10.1016/j.catena.2011.03.012>.
- 633 Jonsson, A., Karlsson, J., Jansson, M., 2003. Sources of carbon dioxide supersaturation in  
634 clearwater and humic lakes in northern sweden. *Ecosystems* 6, 224–235. [https://doi.org/](https://doi.org/10.1007/s10021-002-0200-y)  
635 [10.1007/s10021-002-0200-y](https://doi.org/10.1007/s10021-002-0200-y).
- 636 Kamjunke, N., Buettner, O., Jaeger, C.G., Marcus, H., Von Tuempling, W., Halbedel, S.,  
637 Norf, H., Brauns, M., Baborowski, M., Wild, R., Borchardt, D., Weitere, M., 2013.  
638 Biogeochemical patterns in a river network along a land use gradient. *Environ. Monit.*  
639 *Assess.* 185, 9221–9236. <https://doi.org/10.1007/s10661-013-3247-7>.
- 640 Kaushal, S.S., Delaney-Newcomb, K., Findlay, S.E.G., Newcomer, T.A., Duan, S., Pennino,  
641 M.J., Sviridchi, G.M., Sides-Raley, A.M., Walbridge, M.R., Belt, K.T., 2014.  
642 Longitudinal patterns in carbon and nitrogen fluxes and stream metabolism along an  
643 urban watershed continuum. *Biogeochemistry* 121, 23–44.  
644 <https://doi.org/10.1007/s10533-014-9979-9>.
- 645 Kemenes, A., Forsberg, B.R., Melack, J.M., 2011. CO<sub>2</sub> emissions from a tropical  
646 hydroelectric reservoir (balbina, brazil). *J. Geophys. Res-Biogeosci.* 116, G03004.  
647 <https://doi.org/10.1029/2010jg001465>.
- 648 Kortelainen, P., Rantakari, M., Huttunen, J.T., Mattsson, T., Alm, J., Juutinen, S., Larmola,  
649 T., Silvola, J., Martikainen, P.J., 2006. Sediment respiration and lake trophic state are  
650 important predictors of large CO<sub>2</sub> evasion from small boreal lakes. *Glob. Chang. Biol.* 12,  
651 1554–1567. <https://doi.org/10.1111/j.1365-2486.2006.01167.x>.
- 652 Kosten, S., Roland, F., Da Motta Marques, D.M.L., Van Nes, E.H., Mazzeo, N., Sternberg,  
653 L.d.S.L., Scheffer, M., Cole, J.J., 2010. Climate-dependent CO<sub>2</sub> emissions from lakes.  
654 *Global Biogeochem. Cycles* 24. <http://doi.org/10.1029/2009gb003618>.
- 655 Kunz, M.J., Wueest, A., Wehrli, B., Landert, J., Senn, D.B., 2011. Impact of a large tropical  
656 reservoir on riverine transport of sediment, carbon, and nutrients to downstream wetlands.  
657 *Water Resour. Res.* 47. <http://doi.org/10.1029/2011wr010996>.
- 658 Kutzbach, L., Wille, C., Pfeiffer, E.M., 2007. The exchange of carbon dioxide between wet  
659 arctic tundra and the atmosphere at the lena river delta, northern siberia. *Biogeosciences*  
660 4, 869–890. <http://doi.org/10.5194/bg-4-869-2007>.
- 661 Lai, L., Huang, X., Yang, H., Chuai, X., Zhang, M., Zhong, T., Chen, Z., Chen, Y., Wang,  
662 X., Thompson, J., R., 2016. Carbon emissions from land-use change and management in  
663 China between 1990 and 2010. *Sci. Adv.* 2(11), e1601063. [http://doi.org/10.1126/](http://doi.org/10.1126/sciadv.1601063)  
664 [sciadv.1601063](http://doi.org/10.1126/sciadv.1601063).
- 665 Lehner, B., Liermann, C.R., Revenga, C., Voeroesmarty, C., Fekete, B., Crouzet, P., Doell,  
666 P., Endejan, M., Frenken, K., Magome, J., Nilsson, C., Robertson, J.C., Roedel, R.,  
667 Sindorf, N., Wisser, D., 2011. High-resolution mapping of the world's reservoirs and  
668 dams for sustainable river-flow management. *Front. Ecol. Environ.* 9, 494–502.  
669 <http://doi.org/10.1890/100125>.
- 670 Li, S., Lu, X.X., 2012. Uncertainties of carbon emission from hydroelectric reservoirs. *Nat.*  
671 *Hazards* 62, 1343–1345. <http://doi.org/10.1007/s11069-012-0127-3>.

- 672 Li, S., Lu, X.X., Bush, R.T., 2013. CO<sub>2</sub> partial pressure and CO<sub>2</sub> emission in the lower  
673 mekong river. *J. Hydrol.* 504, 40–56. <http://doi.org/10.1016/j.jhydrol.2013.09.024>.
- 674 Li, S.Y., Zhang, Q.F., 2014. Partial pressure of CO<sub>2</sub> and CO<sub>2</sub> emission in a monsoon-driven  
675 hydroelectric reservoir (Danjiangkou Reservoir), China. *Ecol. Eng.* 71, 401–414.  
676 <https://doi.org/10.1016/j.ecoleng.2014.07.014>.
- 677 Li, Z., Zhang, Z., Lin, C., Chen, Y., Wen, A., Fang, F., 2016. Soil-air greenhouse gas fluxes  
678 influenced by farming practices in reservoir drawdown area: A case at the three gorges  
679 reservoir in china. *J. Environ. Manag.* 181, 64–73. <http://doi.org/10.1016/j.jenvman.2016.05.080>.
- 681 Li, S.Y., Bush, R.T., Santos, I.R., Zhang, Q.F., Song, K.S., Mao, R., Wen, Z.D., Lu, X.X.,  
682 2018. Large greenhouse gases emissions from China's lakes and reservoirs. *Water Res.*  
683 147, 13–24. <https://doi.org/10.1016/j.watres.2018.09.053>.
- 684 Li, Y., Yang, H., Zhang, L., Yang, X., Zang, H., Fan, W., Wang, G., 2020a. The  
685 spatiotemporal variation and control mechanism of surface *p*CO<sub>2</sub> in winter in Jiaozhou  
686 Bay, China. *Cont. Shelf Res.* 206. <https://doi.org/10.1016/j.csr.2020.104208>.
- 687 Li, Y., Zhang, L., Xue, L., Fan, W., Liu, F., Yang, H., 2020b. Spatial Variation in Aragonite  
688 Saturation State and the Influencing Factors in Jiaozhou Bay, China. *Water* 12(3), 825.  
689 <https://doi.org/10.3390/w12030825>.
- 690 Liu, H.P., Zhang, Q.Y., Katul, G.G., Cole, J.J., Chapin, F.S., MacIntyre, S., 2016. Large CO<sub>2</sub>  
691 effluxes at night and during synoptic weather events significantly contribute to CO<sub>2</sub>  
692 emissions from a reservoir. *Environ. Res. Lett.* 11(6), 8–10. [https://doi.org/1088/1748-](https://doi.org/1088/1748-9326/11/6/064001)  
693 [9326/11/6/064001](https://doi.org/1088/1748-9326/11/6/064001).
- 694 Liu, Z., Guan, D.B., Crawford-Brown, D., Zhang, Q., He, K.B., Liu, J.G., 2013. A low-  
695 carbon road map for China. *Nature* 500(7461), 143–145. <https://doi.org/10.1038/500143a>.
- 696 Marescaux, A., Thieu, V., Garnier, J., 2018. Carbon dioxide, methane and nitrous oxide  
697 emissions from the human-impacted Seine watershed in France. *Sci. Total Environ.* 643,  
698 247–259. <https://doi.org/10.1016/j.scitotenv.2018.06.151>.
- 699 Matthews, C.J.D., Joyce, E.M., St Louise, V.L., Schiff, S.L., Venkiteswaran, J.J., Hall, B.D.,  
700 Bodaly, R.A., Beaty, K.G., 2005. Carbon dioxide and methane production in small  
701 reservoirs flooding upland boreal forest. *Ecosystems* 8, 267–285. [http://doi.org/](http://doi.org/10.1007/s10021-005-0005-x)  
702 [10.1007/s10021-005-0005-x](http://doi.org/10.1007/s10021-005-0005-x).
- 703 Natchimuthu, S., Selvam, B.P., Bastviken, D., 2014. Influence of weather variables on  
704 methane and carbon dioxide flux from a shallow pond. *Biogeochemistry* 119, 403–413.  
705 <http://doi.org/10.1007/s10533-014-9976-z>.
- 706 Natchimuthu, S., Sundgren, I., Gålfalk, M., Klemedtsson, L., Crill, P., Danielsson, Å.,  
707 Bastviken, D., 2016. Spatio-temporal variability of lake CH<sub>4</sub> fluxes and its influence on  
708 annual whole lake emission estimates. *Limnol. Oceanogr.* 61, S13–S26.  
709 <https://doi.org/10.1002/lno.10222>.
- 710 Ni, M., Li, S., Luo, J., Lu, X., 2019. CO<sub>2</sub> partial pressure and CO<sub>2</sub> degassing in the daning  
711 river of the upper yangtze river, china. *J. Hydrol.* 569, 483–494. [https://doi.org/](https://doi.org/10.1016/j.jhydrol.2018.12.017)  
712 [10.1016/j.jhydrol.2018.12.017](https://doi.org/10.1016/j.jhydrol.2018.12.017).
- 713 Nilsson, C., Reidy, C.A., Dynesius, M., Revenga, C., 2005. Fragmentation and flow  
714 regulation of the world's large river systems. *Science* 308, 405–408.  
715 <http://doi.org/10.1126/science.1107887>.

716 Outram, F.N., Hiscock, K.M., 2012. Indirect nitrous oxide emissions from surface water  
717 bodies in a lowland arable catchment: A significant contribution to agricultural  
718 greenhouse gas budgets? *Environ. Sci. Technol.* 46, 8156–8163. [http://doi.org/](http://doi.org/10.1021/es3012244)  
719 [10.1021/es3012244](http://doi.org/10.1021/es3012244).

720 Pacheco, F.S., Soares, M.C.S., Assireu, A.T., Curtarelli, M.P., Roland, F., Abril, G., Stech,  
721 J.L., Alvala, P.C., Ometto, J.P., 2015. The effects of river inflow and retention time on  
722 the spatial heterogeneity of chlorophyll and water-air CO<sub>2</sub> fluxes in a tropical hydropower  
723 reservoir. *Biogeosciences* 12, 147–162. <http://doi.org/10.5194/bg-12-147-2015>.

724 Pérez, C.A., Degrandpre, M.D., Lagos, N.A., Saldías, G.S., Cascales, E.-K., Vargas, C.A.,  
725 2015. Influence of climate and land use in carbon biogeochemistry in lower reaches of  
726 rivers in central southern chile: Implications for the carbonate system in river-influenced  
727 rocky shore environments. *J. Geophys. Res-Bioge.* 120, 673–692. [http://doi.org/](http://doi.org/10.1002/2014jg002699)  
728 [10.1002/2014jg002699](http://doi.org/10.1002/2014jg002699).

729 Pugh, T.A.M., Arneeth, A., Olin, S., Ahlstrom, A., Bayer, A.D., Goldewijk, K.K., Lindeskog,  
730 M., Schurgers, G., 2015. Simulated carbon emissions from land-use change are  
731 substantially enhanced by accounting for agricultural management. *Environ. Res. Lett.*  
732 10. <http://doi.org/10.1088/1748-9326/10/12/124008>.

733 Raymond, P.A., Cole, J.J., 2003. Increase in the export of alkalinity from north america's  
734 largest river. *Science* 301, 88–91. <http://doi.org/10.1126/science.1083788>.

735 Raymond, P.A., Hartmann, J., Lauerwald, R., Sobek, S., Mcdonald, C., Hoover, M., Butman,  
736 D., Striegl, R., Mayorga, E., Humborg, C., Kortelainen, P., Duerr, H., Meybeck, M.,  
737 Ciais, P., Guth, P., 2014. Global carbon dioxide emissions from inland waters. *Nature*  
738 503, 355. <http://doi.org/10.1038/nature13142>.

739 Roland, F., Vidal, L.O., Pacheco, F.S., Barros, N.O., Assireu, A., Ometto, J.P.H.B.,  
740 Cimleris, A.C.P., Cole, J.J., 2010. Variability of carbon dioxide flux from tropical  
741 (Cerrado) hydroelectric reservoirs. *Aquat. Sci.* 72, 283–293. [https://doi.org/10.1007/](https://doi.org/10.1007/s00027-010-0140-0)  
742 [s00027-010-0140-0](https://doi.org/10.1007/s00027-010-0140-0).

743 Rosenberg, D.M., Mccully, P., Pringle, C.M., 2000. Global-scale environmental effects of  
744 hydrological alterations: Introduction. *Bioscience* 50, 746–751. [http://doi.org/10.1641/](http://doi.org/10.1641/0006-3568(2000)050[0746:Gseeoh]2.0.Co;2)  
745 [0006-3568\(2000\)050\[0746:Gseeoh\]2.0.Co;2](http://doi.org/10.1641/0006-3568(2000)050[0746:Gseeoh]2.0.Co;2).

746 Schilder, J., Bastviken, D., van Hardenbroek, M., Kankaala, P., Rinta, P., Stotter, T., Heiri,  
747 O., 2013. Spatial heterogeneity and lake morphology affect diffusive greenhouse gas  
748 emission estimates of lakes. *Geophys. Res. Lett.* 40, 5752–5756. [https://doi.org/](https://doi.org/10.1002/2013GL057669)  
749 [10.1002/2013GL057669](https://doi.org/10.1002/2013GL057669).

750 Scofield, V., Melack, J.M., Barbosa, P.M., Amaral, J.H.F., Forsberg, B.R., Farjalla, V.F.,  
751 2016. Carbon dioxide outgassing from amazonian aquatic ecosystems in the negro river  
752 basin. *Biogeochemistry* 129, 77–91. <http://doi.org/10.1007/s10533-016-0220-x>.

753 Shi, W., Chen, Q., Yi, Q., Yu, J., Ji, Y., Hu, L., Chen, Y., 2017. Carbon emission from  
754 cascade reservoirs: Spatial heterogeneity and mechanisms. *Environ. Sci. Technol.* 51,  
755 12175–12181. <http://doi.org/10.1021/acs.est.7b03590>.

756 Sobek, S., Tranvik, L.J., Cole, J.J., 2005. Temperature independence of carbon dioxide  
757 supersaturation in global lakes. *Global Biogeochem. Cycles* 19, GB2003.  
758 <http://doi.org/10.1029/2004gb002264>.

- 759 Soumis, N., Lucotte, M., Larose, C., Veillette, F., Canuel, R., 2007. Photomineralization in a  
760 boreal hydroelectric reservoir: A comparison with natural aquatic ecosystems.  
761 *Biogeochemistry* 86, 123–135. <http://doi.org/10.1007/s10533-007-9141-z>.
- 762 St Louis, V.L., Kelly, C.A., Duchemin, E., Rudd, J.W.M., Rosenberg, D.M., 2000. Reservoir  
763 surfaces as sources of greenhouse gases to the atmosphere: A global estimate. *Bioscience*  
764 50, 766–775. [http://doi.org/10.1641/0006-3568\(2000\)050\[0766:Rsasog\]2.0.Co;2](http://doi.org/10.1641/0006-3568(2000)050[0766:Rsasog]2.0.Co;2).
- 765 Tong, C., Wang, W.Q., Zeng, C.S., Marrs, R., 2010. Methane (CH<sub>4</sub>) emission from a tidal  
766 marsh in the min river estuary, southeast china. *J. Environ. Sci. Heal. A.* 45, 506–516.  
767 <http://doi.org/10.1080/10934520903542261>.
- 768 Urabe, J., Iwata, T., Yagami, Y., Kato, E., Suzuki, T., Hino, S., Ban, S., 2011. Within-lake  
769 and watershed determinants of carbon dioxide in surface water: A comparative analysis of  
770 a variety of lakes in the japanese islands. *Limnol. Oceanogr.* 56, 49–60.  
771 <http://doi.org/10.4319/lo.2011.56.1.0049>.
- 772 Varis, O., Kumm, M., Härkönen, S., Huttunen, J.T., 2011. Greenhouse gas emissions from  
773 reservoirs. *Impacts of Large Dams: A Global Assessment*, Springer 69–94.  
774 [https://doi.org/10.1007/978-3-642-23571-9\\_4](https://doi.org/10.1007/978-3-642-23571-9_4).
- 775 Van Bergen, T.J.H.M., Barros, N., Mendonca, R., Aben, R.C.H., Althuisen, I.H.J., Huszar,  
776 V., Lamers, L.P.M., Lurling, M., Roland, F., Kosten, S., 2019. Seasonal and diel variation  
777 in greenhouse gas emissions from an urban pond and its major drivers. *Limnol. Oceanogr.*  
778 64, 2129–2139. <http://doi.org/10.1002/lno.11173>.
- 779 Venkiteswaran, J.J., Schiff, S.L., Wallin, M.B., 2014. Large carbon dioxide fluxes from head-  
780 water boreal and sub-boreal streams. *PLoS One* 9:22–25. [https://doi.org/10.1371/  
781 journal.pone.0101756](https://doi.org/10.1371/journal.pone.0101756).
- 782 Wang, F., Wang, B., Liu, C.-Q., Wang, Y., Guan, J., Liu, X., Yu, Y., 2011. Carbon dioxide  
783 emission from surface water in cascade reservoirs-river system on the maotiao river,  
784 southwest of China. *Atmos. Environ.* 45, 3827–3834. [http://doi.org/10.1016/  
785 j.atmosenv.2011.04.014](http://doi.org/10.1016/j.atmosenv.2011.04.014).
- 786 Wang, X.F., He, Y.X., Yuan, X.Z., Chen, H., Peng, C.H., Yue, J.S., Zhang, Q.Y., Diao, Y.B.,  
787 Liu, S.S., 2017. Greenhouse gases concentrations and fluxes from subtropical small  
788 reservoirs in relation with watershed urbanization. *Atmos. Environ.* 154, 225–235.  
789 <http://doi.org/10.1016/j.atmosenv.2017.01.047>.
- 790 Wanninkhof, R., 1992. Relationship between wind-speed and gas-exchange over the ocean. *J.*  
791 *Geophys. Res-Oceans.* 97, 7373–7382. <http://doi.org/10.1029/92jc00188>.
- 792 Wanninkhof, R., 2014. Relationship between wind speed and gas exchange over the ocean  
793 revisited. *Limnol. Oceanogr-Meth.* 12, 351–362. <http://doi.org/10.4319/lom.2014.12.351>.
- 794 Webb, J.R., Santos, I.R., Tait, D.R., Sippo, J.Z., Macdonald, B.C.T., Robson, B., Maher,  
795 D.T., 2016. Divergent drivers of carbon dioxide and methane dynamics in an agricultural  
796 coastal floodplain: Post-flood hydrological and biological drivers. *Chem. Geol.* 440, 313–  
797 325. <http://doi.org/10.1016/j.chemgeo.2016.07.025>.
- 798 Williams, C.J., Frost, P.C., Morales-Williams, A.M., Larson, J.H., Richardson, W.B.,  
799 Chiandet, A.S., Xenopoulos, M.A., 2016. Human activities cause distinct dissolved  
800 organic matter composition across freshwater ecosystems. *Glob. Chang. Biol.* 22, 613–  
801 626. <http://doi.org/10.1111/gcb.13094>.

- 802 Wilson, B.J., Mortazavi, B., Kiene, R.P., 2015. Spatial and temporal variability in carbon  
803 dioxide and methane exchange at three coastal marshes along a salinity gradient in a  
804 northern gulf of Mexico estuary. *Biogeochemistry* 123, 329–347. [http://doi.org/  
805 10.1007/s10533-015-0085-4](http://doi.org/10.1007/s10533-015-0085-4).
- 806 World Meteorological Organization, 2019. WMO Greenhouse Gas Bulletin No.15.
- 807 Xiao, Q.T., Zhang, M., Hu, Z.H., Gao, Y.Q., Hu, C., Liu, C., Liu, S.D., Zhang, Z., Zhao, J.Y.,  
808 Xiao, W., Lee, X., 2017. Spatial variations of methane emission in a large shallow  
809 eutrophic lake in subtropical climate. *J. Geophys. Res.-Biogeo.* 122, 1597–1614.  
810 <https://doi.org/10.1002/2017jg003805>.
- 811 Xiao, S., Wang, Y., Liu, D., Yang, Z., Lei, D., Zhang, C., 2013. Diel and seasonal variation  
812 of methane and carbon dioxide fluxes at site Guojiaba, the Three Gorges Reservoir. *J.*  
813 *Environ. Sci.* 25, 2065–2071. [https://doi.org/10.1016/s1001-0742\(12\)60269-1](https://doi.org/10.1016/s1001-0742(12)60269-1).
- 814 Xing, Y.P., Xie, P., Yang, H., Ni, L.Y., Wang, Y.S., Tang, W.H., 2004. Diel variation of  
815 methane fluxes in summer in a eutrophic subtropical lake in China. *J. Freshwater Ecol.*  
816 19(4), 639–644. <https://doi.org/10.1080/02705060.2004.9664745>.
- 817 Xing, Y., Xie, P., Yang, H., Ni, L., Wang, Y., Rong, K., 2005. Methane and carbon dioxide  
818 fluxes from a shallow hypereutrophic subtropical Lake in China. *Atmos. Environ.* 39(30),  
819 5532–5540. <https://doi.org/10.1016/j.atmosenv.2005.06.010>.
- 820 Xing, Y.P., Xie, P., Yang, H., Wu, A.P., Ni, L.Y., 2006. The change of gaseous carbon fluxes  
821 following the switch of dominant producers from macrophytes to algae in a shallow  
822 subtropical lake of China. *Atmos. Environ.* 40(40), 8034–8043. [https://doi.org/10.1016/  
823 j.atmosenv.2006.05.033](https://doi.org/10.1016/j.atmosenv.2006.05.033).
- 824 Yang, H., 2014. China must continue the momentum of green law. *Nature* 509, 535–535.  
825 <https://doi.org/10.1038/509535a>.
- 826 Yang, H., Andersen, T., Dörsch, P., Tominaga, K., Thrane, J.-E., Hessen, D.O., 2015.  
827 Greenhouse gas metabolism in Nordic boreal lakes. *Biogeochemistry* 126, 211–225.  
828 <https://doi.org/10.1007/s10533-015-0154-8>.
- 829 Yang, H., Flower, R.J., 2012. Potentially massive greenhouse-gas sources in proposed  
830 tropical dams. *Front. Ecol. Environ.* 10(5), 234–235. <https://doi.org/10.1890/12.WB.014>.
- 831 Yang, H., Flower, R.J., Thompson, J.R., 2013. China's new leaders offer green hope. *Nature*  
832 493(7431), 163–163. <https://doi.org/10.1038/493163d>.
- 833 Yang, H., Huang, X., Thompson, J.R., Flower, R.J., 2015. Enforcement key to China's  
834 environment. *Science* 347(6224), 834–835. [https://doi.org/10.1126/science.347.6224.83  
835 4-d](https://doi.org/10.1126/science.347.6224.834-d).
- 836 Yang, H., Ma, M., Thompson, J.R., Flower, R.J., 2017. Protect coastal wetlands in China to  
837 save endangered migratory birds. *P. Natl. Acad. Sci. USA.* 114(28), E5491–E5492.  
838 <https://doi.org/10.1073/pnas.1706111114>.
- 839 Yang, H., Thompson, J.R., Flower, R.J., 2019. Save horseshoe crabs and coastal ecosystems.  
840 *Science* 366(6467), 813–814. <https://doi.org/10.1126/science.aaz8654>.
- 841 Yang, H., Wright, J.A., Gundry, S.W., 2012a. Boost water safety in rural China. *Nature*  
842 484(7394), 318–318. <https://doi.org/10.1038/484318b>.
- 843 Yang, H., Xie, P., Ni, L., Flower, R.J., 2012b. Pollution in the Yangtze. *Science* 337(6093),  
844 410–410. <https://doi.org/10.1126/science.337.6093.410-a>.

- 845 Yang, H., Xing, Y., Xie, P., Ni, L., Rong, K., 2008. Carbon source/sink function of a  
846 subtropical, eutrophic lake determined from an overall mass balance and a gas exchange  
847 and carbon burial balance. *Environ. Pollut.* 151, 559–568. [https://doi.org/  
848 10.1016/j.envpol.2007.04.006](https://doi.org/10.1016/j.envpol.2007.04.006).
- 849 Yang, P., Zhang, Y., Lai, D.Y.F., Tan, L., Jin, B., Tong, C., 2018. Fluxes of carbon dioxide  
850 and methane across the water-atmosphere interface of aquaculture shrimp ponds in two  
851 subtropical estuaries: The effect of temperature, substrate, salinity and nitrate. *Sci. Total  
852 Environ.* 635, 1025–1035. <https://doi.org/10.1016/j.scitotenv.2018.04.102>.
- 853 Yang, P., Yang, H., Sardans, J., Tong, C., Zhao, G.H., Peñuelas, J., Li, L., Zhang, Y.F., Tan,  
854 L.S., Chun, K.P., Lai, D.Y.F., 2020. Large spatial variations in diffusive CH<sub>4</sub> fluxes from  
855 a subtropical coastal reservoir affected by sewage discharge in southeast China. *Environ.  
856 Sci. Technol.* 54, 22, 14192–14203. <https://doi.org/10.1021/acs.est.0c03431>
- 857 Yoon, T.K., Jin, H., Begum, M.S., Kang, N., Park, J. H., 2017. CO<sub>2</sub> outgassing from an  
858 urbanized river system fueled by wastewater treatment plant effluents. *Environ. Sci.  
859 Technol.* 51, 10459–10467. <https://doi.org/10.1021/acs.est.7b02344>.
- 860 Yu, Z., Wang, D., Li, Y., Deng, H., Hu, B., Ye, M., Zhou, X., Da, L., Chen, Z., Xu, S., 2017.  
861 Carbon dioxide and methane dynamics in a human-dominated lowland coastal river  
862 network (shanghai, china). *Journal of Geophysical Research-Biogeosciences* 122, 1738–  
863 1758. <https://doi.org/10.1002/2017jg003798>.
- 864 Zhang, M., Huang, X., Chuai, X., Yang, H., Lai, L., Tan, J., 2015. Impact of land use type  
865 conversion on carbon storage in terrestrial ecosystems of China: A spatial-temporal  
866 perspective. *Sci. Rep-UK.* 5, 10233. <https://doi.org/10.1038/srep10233>.
- 867 Zhang, Y.F, Yang, P., Yang, H., Tan, L.S, Guo, Q.Q, Zhao, G.H, Li, L., Gao, Y., Tong, C.,  
868 2019. Plot-scale spatiotemporal variations of CO<sub>2</sub> concentration and flux across water-air  
869 interfaces at aquaculture shrimp ponds in a subtropical estuary. *Environ. Sci. Pollut. R.*  
870 26, 5623–5637. <http://doi.org/10.1007/s11356-018-3929-3>.
- 871 Zhao, Y., Wu, B.F., Zeng, Y., 2013. Spatial and temporal patterns of greenhouse gas  
872 emissions from three gorges reservoir of china. *Biogeosciences* 10, 1219–1230.  
873 [http://doi.org/ 10.5194/bg-10-1219-2013](http://doi.org/10.5194/bg-10-1219-2013).
- 874 Zhou, S., He, Y., Yuan, X., Peng, S., Yue, J., 2017. Greenhouse gas emissions from different  
875 land-use areas in the littoral zone of the three gorges reservoir, china. *Ecol. Eng.* 100,  
876 316–324. <http://doi.org/10.1016/j.ecoleng.2017.01.003>.
- 877